Accepted for publication in *The Galapágos: A Natural Laboratory for the Earth Sciences*, AGU Monograph Series, June 2013.

Controls on the hydrological and topographic evolution of shield volcanoes and volcanic ocean islands

Anne J. Jefferson[1], Ken L. Ferrier[2], J. Taylor Perron[3], Ricardo Ramalho[4]

1. Department of Geology, Kent State University, ajeffer9@kent.edu

2. Department of Earth and Planetary Sciences, Harvard University, ferrier@fas.harvard.edu

3. Department of Earth, Atmospheric, and Planetary Sciences, Massachusetts Institute of Technology, perron@mit.edu

4. Institut für Geophysik, Westfälische Wilhelms-Universität, Münster, Germany, ricardo.ramalho@uni-muenster.de

Accepted for publication in *The Galapágos: A Natural Laboratory for the Earth Sciences*, AGU Monograph Series, June 2013.

Controls on the hydrological and topographic evolution of shield volcanoes and volcanic ocean islands

Anne J. Jefferson[1], Ken L. Ferrier[2], J. Taylor Perron[3], Ricardo Ramalho[4]

1. Department of Geology, Kent State University, ajeffer9@kent.edu

2. Department of Earth and Planetary Sciences, Harvard University, ferrier@fas.harvard.edu

3. Department of Earth, Atmospheric, and Planetary Sciences, Massachusetts Institute of Technology, perron@mit.edu

4. Institut für Geophysik, Westfälische Wilhelms-Universität, Münster, Germany, ricardo.ramalho@uni-muenster.de

Abstract

Volcanic ocean islands and shield volcanoes form superb natural experiments for investigating changes in topography and hydrology over geologic time. As volcanoes age, their surfaces evolve from undissected, high-permeability landscapes into deeply dissected, low-permeability terrain. Here we review the tight linkages and co-evolution of topographic and hydrologic processes in volcanic landscapes. We discuss a number of factors that affect rates and patterns of hydrological and topographic co-evolution, including soil development, spatial and temporal variability of water availability, flank collapses, geologic architecture, and the tectonic history of subsidence or uplift. To illustrate the effects of climate on volcanic dissection, we compile a global dataset of volcanic landscapes and ages that suggests that substantial dissection begins between 0.5 and 2 million years after construction, with volcanoes in high precipitation regions tending to become dissected more quickly than those in drier regions. Obtaining a deeper understanding of volcanic landscape evolution will require further research on several topics, such as the sensitivity of river incision to fluctuations in precipitation; the hydrologic responses of soil to chemical weathering and dust deposition; the evolution of chemical and physical erosion rates over a volcano's lifetime; the role of hydrology in triggering of flank collapses; and the extent to which the long-term evolution of an island is determined by the initial and boundary conditions set by geologic structure and regional tectonics.

Keywords

Landscape evolution, hydrologic processes, shield volcanoes, ocean islands, dissection, climate

1. Introduction

As volcanic landscapes transform from bare, undissected surfaces into vegetated landscapes with deeply entrenched river valleys, they form extraordinary natural experiments in landscape evolution, with unparalleled constraints on the timing and form of the initial topography. Volcanic landscapes undergo dramatic topographic changes following construction [*Thouret*, 1999], and they also grow profoundly less permeable [e.g., *Ingebritsen et al.*, 1992], which radically alters the way water moves across the surface and through the subsurface [*Lohse and Dietrich*, 2005; *Jefferson et al.*, 2010]. These topographic and hydrologic changes are closely coupled to one another, and the interplay between them can be understood as a modification of well-constrained initial conditions. As such, volcanic ocean islands and shield volcanoes offer a remarkable opportunity to study the co-evolution of topography and hydrology. These co-evolving processes set the template for ecosystem structure, volcanic hazards, and water availability in volcanic landscapes of all ages. Thus, understanding the processes, patterns, and timescales of volcanic landscape evolution is not only of interest to hydrologists and geomorphologists, but is also important for ecologists interested in understanding species distributions and evolutionary history [*Whittaker et al.*, 2008], for volcanologists assessing risks from lava flows, lahars, or water-magma interactions [e.g., *Fisher*, 1995; *Mastin and Witter*, 2000; *Németh and Cronin*, 2011], and for communities seeking sustainable water supplies [e.g., *Koh et al.*, 2005; *Herrera and Custodio*, 2008; *Carreira et al.*, 2010; *Cruz et al.*, 2011].

Not all volcanic landscapes experience the same processes and trajectories of hydrologic and topographic change. In some parts of the world, occasional intense rainstorms cause torrents of water to cut steep canyons through an otherwise arid landscape [*Mannaerts and Gabriels*, 2000; *Menendez et al.*, 2008]. Elsewhere, gentle rainfall and fog drip may promote soil and vegetation development, even though surface water remains largely absent from the landscape [*Adelinet et al.*, 2008; *Trueman and d'Ozouville*, 2010; *Pryet et al.*, 2012]. Orographic precipitation may cause one side of a volcano to become deeply eroded while the other side retains its initial form [*Wentworth*, 1927; *Stearns*, 1946; *Ferrier et al.*, 2013]. Massive flank collapses may remove large sectors of a volcano and catalyze rapid knickpoint retreat and incision in the remaining landscape [*Lamb et al.*, 2007], and eruption patterns may create substantial spatial variability in permeability [*Izuka and Gingerich*, 2003; *Won et al.*, 2005] that drive different trajectories of landscape evolution. All of these processes act on volcanoes around the world, but their relative importance can vary widely, modifying the timescales and trajectories of topographic and hydrologic evolution and leading to a diversity of volcanic landforms and hydrologic states.

In this paper, we propose a conceptual framework for understanding the major controls on the co-evolution of hydrology and topography of shield volcanoes and volcanic islands, in order to identify the controls and patterns common to all volcanic landscapes, to analyze how the relative importance of those controls in various regions, and to identify fruitful areas for future research. Section 2 presents this conceptual framework and defines the scope of co-evolutionary processes. In section 3, we assemble a global dataset of shield volcanoes and ocean islands, which we use to assess the extent to which climate sets the pace of volcanic landscape evolution. In section 4, we review observations from diverse volcanic landscapes to illustrate the various controls on their evolution, beginning with sites that clearly demonstrate the hydrologic and geomorphic responses to climate and then shifting to sites that demonstrate the effects of non-climatic factors such as subsurface volcanic architecture and tectonics.

2. A general framework for volcanic landscape evolution

Volcanic landscape evolution is generally defined by changes over time in the way water is routed over and through the landscape and the concomitant changes in the landscape's topography. For volcanic landscapes, as in most others, hydrologic processes are the dominant drivers of landscape evolution, and topographic changes effected by water in turn affect the hydrologic processes. Partitioning of water between runoff and groundwater is controlled by vegetative cover, soil characteristics, bedrock transmissivity, slope, and patterns of precipitation and evapotranspiration [*Dunne and Leopold*, 1978]. As a landscape ages, each of these factors may change. If they change in the direction of increasing surface runoff, streams grow more capable of incising and dissecting the landscape, which further changes the distribution of water between the surface and subsurface. Thus, there can be feedbacks between hydrology and topography, as well as more complicated feedbacks involving soils, plants, and climate.

In the simplest sense, the topographic development and hydrologic processes operating on a volcanic landscape can be conceived of as a function of water availability and the age of the volcanic bedrock. The amount, timing, and spatial distribution of water available for surface and subsurface flow control the potential for weathering and fluvial erosion, while age is a measure of the timescale over which water and the volcanic landscape have interacted. Volcanic landscapes form a special case for studying co-evolution of hydrology and topography, because few other landscapes undergo such dramatic changes in permeability from their origins as barren rock. There can also be competition in volcanic landscapes between water-driven erosion and constructive and destructive volcanic and tectonic processes. For example, a stream valley may be filled by a lava flow, and a dike injection may disrupt groundwater flowpaths.

On volcanoes, distinctive topographic changes over time can be dramatic enough to qualitatively distinguish stages of landscape evolution from topographic maps and imagery (Figure 1). In recognition of the striking topographic differences among volcanoes, in this paper we adopt the following qualitative classification of volcanic landscapes, based on a visual assessment of the degree of topographic dissection. Undissected volcanoes are easily recognizable by their constructional volcanic topography, an absence of surface drainage networks [*Wentworth*, 1927; *Stearns*, 1942] and extremely high bedrock permeability (10^{-9} to 10^{-11} m^2) [*Davis*, 1969]. Weakly dissected volcanoes have incipient drainage networks with low drainage density and little tributary development, and lack deep valleys. In a few cases, weakly dissected volcanoes may have valleys along their periphery but also have a large undissected caldera or summit area. Substantially dissected volcanoes have higher drainage density, with fluvial valleys that penetrate inland to the central portion of the volcano. Eventually, the only remnant of the volcano's initial constructional surface may be a small, high elevation, central plateau [*Wentworth*, 1927].

Stages of hydrological evolution cannot be directly observed remotely, but they can be estimated based on the stages of topographic landscape evolution. On undissected volcanoes, most precipitation returns to the atmosphere through evapotranspiration or infiltrates to recharge groundwater, leaving no obvious drainage network. On weakly dissected volcanoes, some precipitation in excess of evapotranspiration is routed through surface drainage, but low drainage density and absence of significant incision suggests that groundwater drainage is likely still a dominant hydrologic process. The presence of substantial dissection indicates that fluvial processes have had enough water and time to erode substantial rock volumes, and suggests that groundwater drainage may be of secondary importance in terms of water routing [*Jefferson et al.*, 2010].

We emphasize that this classification scheme is qualitative, and that quantitative metrics for topography (e.g., drainage density) and hydrology (e.g., rates of runoff and groundwater recharge) will be required to better constrain models of the co-evolution of volcanic topography and hydrology. Such quantities are, however, difficult to obtain with the low-resolution topographic data and sparse hydrologic measurements currently available for many volcanic islands. For this reason, we limit ourselves to this qualitative characterization of the degree of topographic development, and note that as remotely sensed data and global mapping efforts [e.g., *Gleeson et al.*, 2011] improve in spatial resolution, quantification may become possible even where field data remains limited.

3. Insights from a global compilation of volcanic ocean islands and shield volcanoes

To test the idea that topographic dissection of shield volcanoes and volcanic ocean islands is a function of landscape age and water availability, we compiled a global database of 97 ocean island and shield volcanoes with published ages and annual precipitation rates, and visually assessed the intensity of dissection of the volcanic edifice. Details of the selected volcanoes, calculations, and data sources are in the Appendix.

Water availability is most easily quantified using a metric related to precipitation, since that is the dominant input of water to a volcanic landscape. Precipitation can vary strongly across seasons and across the landscape, but few volcanoes have extensive meteorological observation networks that would permit characterization of their climatic variability in time and space. We report instead a representative precipitation rate (m/y) for each volcano based on historical data, which corresponds to the best estimate of the spatially averaged mean annual precipitation for a volcano. These estimates of spatially-averaged mean annual precipitation are from reported averages in the literature, WMO station records [*WMO*, 1998], existing spatial interpolation schemes [e.g., *Daly et al.*, 1994; *Daly et al.*, 2002; *Trueman and d'Ozouville*, 2010], or medians of reported values from multiple stations. However, the representative precipitation rate may still be an underestimate in some regions where adequate data do not exist for areas of maximum rainfall, high elevations, or windward slopes. Details of the data sources and calculation methods are given in the Appendix.

The cooling age of volcanic bedrock can often be dated, and isotopic ages and historical eruption data are readily available for many volcanoes around the world. Thus, the time over which water and the volcanic landscape have interacted can be quantified for an individual lava flow or deposit, or at the landscape scale, by a representative age of volcanic activity that produced the bedrock exposed nearest the present land surface. Given the global overview in this compilation, we calculated a single *representative age* (ka) for each volcano, on the basis of (1) a reported average or shield age, (2) a median of the oldest and youngest dates available, or (3) the reported age, if only a single date was available. In regions where multiple dates and geologic mapping are available, it is possible to more rigorously calculate a representative age based on a weighted average of map unit ages [e.g., *Jefferson et al.*, 2010] or to assign multiple ages to each island. Unfortunately, these data are not available for every volcano in the compilation and such calculations are beyond the scope of the present work.

The 97 volcanoes included in this analysis are found in 14 different geographic regions, range in representative age from 500 years to 10.7 million years old (Ma), and span representative precipitation rates from 0.07 to 5.46 m yr^{-1} (Figure 2, Appendix). We classified 53 volcanoes as undissected/weakly dissected (Figure 3), using the criteria described above (Section 2). More substantial dissection was apparent in 41 volcanoes in the dataset and 3 volcanoes were best described as razed edifices, partially or completely truncated by marine erosion and later exposed by uplift.

This compilation suggests volcanic landscape evolution occurs over timescales that are globally broadly consistent, but that precipitation may influence the onset of substantial dissection within those broad timescales (Figure 3). On volcanoes less than 500 thousand years old (ka), there tends to be little or no dissection of the landscape. The 500 ka lag between volcanic landscape construction and substantial dissection may reflect time during which hydrological changes occur through "hidden" processes of soil development and dust deposition that do little to modify the topography. These processes promote hydrologic changes such as reductions in permeability that may be prerequisites for dissection. Also, within the first 500 thousand years (kyr), chemical erosion may remove substantial mass from a volcanic edifice before physical erosion begins to dissect the terrain. By 2000 ka, most volcanoes, even in arid environments, are substantially dissected.

Between 500 and 2000 ka, there is a transition between weak dissection and substantial dissection, during which dissection proceeds into the core of the volcano and erosional rather than constructional topography starts to dominate. The effect of precipitation is apparent in this transitional age range. There are four volcanoes with ages between 500 and 1000 ka that receive >2 m yr^{-1} representative precipitation. Three of these four volcanoes are substantially dissected. In contrast, there are seven volcanoes in the same age range that receive <2 m yr^{-1} representative precipitation. Of these, six are undissected or weakly dissected, and only one is substantially dissected. Five more volcanoes with ages between 1000 and 2000 ka receive >2 m yr^{-1} representative precipitation, and all are substantially dissected. In the same age range, eight volcanoes receiving <2 m yr^{-1} representative precipitation are undissected or weakly dissected, and three are substantially dissected. The present dataset is limited by the simplifying choices of a single age and precipitation rate, as well as the use of a qualitative index of dissection, but there is a plausible physical mechanism linking precipitation and dissection timescales. Precipitation is a proxy for water available to run off and dissect the landscape, so wetter volcanic landscapes may become dissected more quickly than drier ones, after an initial period of soil development and permeability reduction.

The utility of the simplified, global analysis (Figure 3) is to identify the geographic regions, precipitation rates, and age classes where interesting phenomena occur so that a more detailed and process-based analysis can occur. We can expand on the simple conceptualization of water availability and age as the primary controls on the landscape evolution of a volcano, by refining that idea with other significant factors affecting the evolution of volcanic hydrology and topography:

A. Soil development and dust deposition set the stage for landscape dissection
B. Chemical and physical erosion rates change throughout landscape evolution
C. Precipitation rate affects erosion and soil development
D. Flank collapses can hasten topographic dissection
E. Volcanic architecture and tectonics constrain the patterns of landscape evolution

The remainder of this paper is dedicated to exploring these significant factors influencing hydrologic and topographic evolution (Section 4), briefly highlighting some other potential influences on volcanic landscape evolution (Section 5), and suggesting open research questions. We use studies and observations from around the world, but draw heavily from the Galápagos, Cape Verde, and Hawaiian islands as contrasting examples of volcanic ocean island landscapes.

4. Phenomena driving landscape evolution

4A. Soil development and dust deposition set the stage for landscape dissection

The hydrologic evolution of a volcanic landscape is affected by the evolution of its vegetation and soils. On young basalts, dissolution is enhanced by secretions by symbiotic microbes on plant roots [*Berner and Cochran*, 1998]. Organic matter can be a large fraction of young lava soils (~38-84%), as plant roots and soil organic matter interweave through vesicles and rock fragments, which helps retain water near the land surface [*Vaughan and McDaniel*, 2009]. Vegetation first colonizes the edges of young lava flows, possibly from pre-existing habitats not overrun by lava flows [*Inbar*, 1994; *Inbar et al.*, 1995]. Trees that overhang lava margins drop leaves, needles, and branches onto the flow. In the Oregon High Cascades, on lava less than 5000 years old, vegetation density increases toward the flow edges [*Jefferson et al.*, 2006] and lava flow levees are preferentially colonized because of their ability to retain moisture and proximity to seed sources [*Deligne*, 2012].

Rates of plant and soil development are controlled both by the texture of the substrate and the local climate. In Hawaii, the weathering front propagates downward faster on a'a than pahoehoe flows and soil development initially occurs in fine tephra and crevices around a'a clinkers [*Porder et al.*, 2007]. This has been attributed to the lower permeability and surface area of pahoehoe relative to a'a lava. However, at Craters of the Moon in Idaho, soil and vegetation develop in fractures or crevices in the lava surface, and soil is more abundant on paehoehoe than a'a lava [*Vaughan and McDaniel*, 2009]. There, the slower rate of development on a’a is attributed to greater downward movement of deposited organic and mineral material through fractures, thus requiring greater time and input to develop soil and vegetation on the lava surface. The differences in soil development between Hawaii and Idaho may reflect differences in climate. In the warm, wet Hawaiian Islands, the greater permeability of a’a may afford greater rates of chemical weathering, whereas in cool, dry Idaho, water retention near the surface may be more crucial for plant and soil development.

A number of studies have investigated the evolution of Hawaiian soils by examining soils developed on bedrock of different ages across the Hawaiian Islands [*Chadwick et al.*, 1999; *Vitousek et al.*, 2003; *Porder et al.*, 2007]. These studies have compared soils developed on substrates as young as 300 years on the Big Island of Hawai‘i and as old as 4.1 Ma on Kaua‘i, and their observations show that Hawaiian soil mineralogy changes dramatically over time. The youngest soils in this chronosequence show few signs of chemical weathering and have a coarse texture that reflects the scoria-rich parent rock. Intermediate-age soils, by contrast, are highly weathered andisols with abundant non-crystalline minerals that adsorb phosphorus and complex organic matter, which help maintain soil fertility. The oldest soils are yet more weathered than the intermediate-age soils, and are dominated by Fe- and Al-oxides that lack the capacity to retain or supply nutrients [*Chadwick et al.*, 1999].

These changes in soil mineralogy produce concomitant changes in soil hydrology. *Lohse and Dietrich* [2005] found that the youngest soil (on 300 ya bedrock) in the

Hawaiian chronosequence had a high vertical hydraulic conductivity resulting from its coarse texture, shallow thickness (38 cm), and minimal horizonation. The oldest soil (on 4.1 Ma bedrock), by contrast, was thick (120 cm) and deeply weathered, with a plinthite layer overlying several clay-rich soil horizons. These low-conductivity horizons inhibit vertical water transport and promote lateral transport of water in the oldest soil [*Lohse and Dietrich*, 2005]. In other volcanic environments, similar soil mineralogy and hydrology changes have been observed in soil chronosequences. For basalts in the Pinacate volcanic field in arid Sonora, Mexico, the clay percentage in soil increases linearly with lava age from 200 ka to 1200 ka [*Slate et al.*, 1991]. Andisols have high water retention, with young andisols having permeability (10^{-12} to 10^{-14} m^2) comparable to basalt lava. Like soils formed on lava, as ash-based soils age and weathering products accumulate, water retention increases and permeability decreases [*Nanzyo et al.*, 1993].

Soil development is often accompanied by external inputs of wind-blown loess and wet or dry deposition of dust. Such eolian inputs may be particularly important to the topographic and hydrologic development of volcanic landscapes in arid and semi-arid regions. Fine sediments can clog pores and fractures in lava surfaces, fill swales and topographic depressions [*Eppes and Harrison*, 1999], and form a mantle over volcanic deposits [*Dohrenwend et al.*, 1987]. Young lava flows are effective traps of eolian material because of their high surface roughness and lack of runoff [*Wells et al.*, 1985]. Over time such fine grained sediments may smooth topography and promote surface drainage development by lowering the infiltration capacity of the land surface. The permeability of loess (10^{-12} to 10^{-16} m^2) is several orders of magnitude lower than those of young basalts (10^{-9} to 10^{-11} m^2). On Quaternary basaltic lava fields in California and Nevada, channel incision occurs through the 1-3 m thick fine-grained eolian mantle, but rarely exposes the underlying basalt, even though the lava topography controls the network structure [*Dohrenwend et al.*, 1987].

The importance of eolian processes in soil development in a particular area depends on the local rates of dust deposition, soil production, and soil erosion [*Brimhall et al.*, 1988]. On ocean islands remote from eolian sources, dust fluxes can be 100-1000 times lower than in continental settings [*Kurtz et al.*, 2001]. However, even on ocean islands, dust fluxes can be significant contributors to soil development. Dust flux increases with elevation and rainfall on Hawaii, with accumulation ranging from 330 to 2000 tons ha^{-1} on a 170,000 year old a'a flow. The correlation between dust flux and rainfall has been attributed to dust as condensation nuclei for raindrops [*Porder et al.*, 2007]. On Kohala, where soils have developed on quartz-free basalts over >150 kyr, quartz grains from Asia form up to 30% of the upper 50 cm of the soil [*Kurtz et al.*, 2001]. Silica-rich dust does not weather as rapidly as mafic ash and tephra, so accumulated dust can become a progressively larger component of the soil as chemical weathering preferentially depletes the soil of its other components [*Porder et al.*, 2007]. Tephra deposits can also speed the development of soils and vegetation on young lava flows. Recent work in the Oregon Cascades has shown that juxtaposition of barren surfaces and mature forests on lava flows of similar age can be attributed to syn- and post-eruptive tephra fall of fine materials on which plant colonization could rapidly occur [*Deligne et al.*, 2012].

As valleys propagate into volcanic interiors, gently sloping surfaces are replaced by steep hillslopes and deep valley networks. In the Hawaiian Islands, as well as some other volcanic landscapes, soils on remnant surfaces are dominated by clays and inert oxides and have low hydraulic conductivities [e.g., *Chadwick et al.*, 1999; *Lohse and Dietrich*, 2005]. By contrast, physical erosion of soils on steep hillslopes sweeps away weathered soils and promotes the production of new, less weathered soil [e.g., *Heimsath et al.*, 1997; *Ferrier and Kirchner*, 2008]. The juxtaposition of remnant surfaces and steep-sided valleys results in a patchwork distribution of soils on volcanic islands, with old, low-gradient, low-permeability soils interspersed between young, high-gradient, higher-permeability soils [*Vitousek et al.*, 2003]. As river valleys expand, the area dominated by steep hillslopes increases at the expense of low-gradient remnant surfaces, with young soils becoming more dominant as remnant surfaces are eroded away. Thus, the progressive fluvial dissection of volcanic islands affects island hydrology by changing how water is routed through the landscape, and by changing spatial patterns in soil hydrologic properties.

As soil development, rock weathering, and external sediment deposition proceed, a volcanic landscape becomes more erodible through the generation of unconsolidated material and weakening of rock, and it simultaneously becomes more capable of fluvial erosion as more water is routed along shallow subsurface or surface flowpaths and forms channels. Connecting the soil profile changes described above with landscape-scale development of drainage networks is a research area where more work is needed. What soil structures, thickness, and permeability are required to route water laterally rather than vertically down to a depth where it recharges bedrock groundwater? At what stage of soil development do channels begin to form on volcanic landscapes?

4B. Chemical and physical erosion rates change throughout landscape evolution

The co-evolution of volcanic topography and hydrology affects the relative rates of chemical and physical erosion from island interiors to the ocean. Immediately after construction of the volcano surface, hillslopes are dominated by bare, fractured, highly permeable rock. Any rain falling on these hillslopes percolates quickly into the subsurface and does not concentrate into surface channels. During this early stage, fluvial erosion of solids and solutes is slow, because rivers are scarce. Mechanical weathering can act to smooth the land surface, but does not result in mass loss unless surface runoff can transport the weathered materials away from the volcanic landscape. At the same time, subsurface chemical erosion progresses quickly as groundwater passes through the highly permeable and chemically reactive bedrock. High-temperature water-rock interactions and long subsurface residence times can further enhance chemical erosion rates [*Rad et al.*, 2011]. *Rad et al.* [2007] estimated subsurface chemical erosion rates from measurements of groundwater solute concentrations and estimates of groundwater recharge on the volcanic islands of Guadeloupe, Martinique, and Réunion. They then compared these estimates to measurements of fluvial chemical erosion rates, and suggested that subsurface chemical erosion fluxes outpaced surface chemical erosion rates on these islands by a factor of 2-5. *Schopka and Derry* [2012] carried out a similar analysis on Hawaii and estimated that subsurface chemical erosion fluxes there were 15 times faster than surface fluvial chemical erosion fluxes. Given the lack of surface dissection at this early stage of landscape evolution, subsurface chemical erosion appears to be the primary means of mass transfer from young island interiors to the ocean.

Chemical weathering rates in volcanic landscapes are affected by a number of factors, including mineral supply rates to the weathering zone, precipitation, temperature, vegetation, glacial cover, and rock age, and mineral dissolution kinetics [*Gislason et al.*, 1996; *Benedeti et al.*, 2003; *Pokrovsky et al.*, 2005]. On Hawaii, mass loss via chemical weathering proceeds quickly for the first 10,000 to 20,000 years after lava emplacement, but then rates of mass loss slow at later times [*Vitousek*, 2004; *Porder et al.*, 2007].

As volcanic landscapes grow older, physical erosion of the land surface becomes the dominant mass flux. Hillslope surfaces grow less permeable as soils develop, and surface runoff becomes stronger, which drives channel incision and fluvial transport. Measurements of erosional fluxes on volcanic islands at this stage (Figure 4) show that chemical erosion rates are generally a small fraction of total erosion rates (i.e., the sum of chemical and physical erosion rates). In the measurements compiled in Figure 4, chemical erosion rates comprise on average only 9% of the total erosion rates. We note that the chemical erosion rates in Figure 4 were determined from fluvial solute fluxes, and therefore underestimate total chemical erosion rates because they do not include subsurface chemical erosion fluxes that leave islands in groundwater. However, even if subsurface chemical erosion rates at those sites were several times larger than surface chemical erosion rates, the sum of surface and subsurface chemical erosion fluxes would still be smaller than the surface physical erosion rates at all but two sites. Figure 4 also shows that chemical erosion rates on volcanic islands tend to increase with total erosion rates. This suggests that, once volcanic islands progress beyond their earliest stage of development, there is a close connection between physical and chemical erosion on volcanic islands. In this respect, after their initial stage of development, volcanic islands behave similarly to many continental settings, in which chemical erosion rates are often closely coupled to physical erosion rates [*Riebe et al.*, 2004; *West et al.*, 2005], possibly because physical erosion rates control the supply of fresh, unweathered material to the soil.

4C. Precipitation rate affects erosion and soil development

Volcanic edifices protruding into the atmosphere cause air masses to move up and over them, producing orographic precipitation on their windward sides and a rain shadow on their leeward sides. The upper elevations on the windward side of a volcano can receive much more precipitation than lower elevations or the leeward side, though maximum rainfall does not always correspond with peak elevations. Strong precipitation asymmetry is evident in many ocean island and arc settings, including the Hawaiian Islands and Oregon Cascades [*PRISM*, 2012], and each of these regions displays asymmetry in landscape dissection. An extreme case is Piton de la Fournaise, where annual precipitation rates range from <1 m yr^{-1} to >10 m yr^{-1} [*Violette et al.*, 1997]. Spatial variation in precipitation may have significant consequences for hydrology and landscape evolution, and can be analyzed by sub-dividing a volcano by precipitation and age and quantifying dissection in terms of drainage density, incision depth, or eroded volume. Such an analysis at the global scale is beyond the scope of this paper, but has been undertaken for individual islands [e.g., *Menendez et al.*, 2008; *Ferrier et al.*, 2013].

Evidence for climatic influences on volcanic island topography can be found on the Hawaiian island of Kauaʻi, which is roughly 50 km in diameter, has a maximum elevation of 1593 m, and is the second oldest of the major Hawaiian islands (Figure 5). Superimposed on the island is one of Earth's steepest rainfall gradients, with mean annual precipitation rates as high as 9.5 m yr^{-1} on the island's high-altitude central plateau (peak elevation 1598 m), and as low as 0.5 m yr^{-1} on Kauaʻi's low-lying southwestern coast. Kauaʻi's large rainfall gradient and small lithologic variations make it an exceptional natural laboratory for investigating how erosion rates on volcanic islands are influenced by rainfall rates.

Ferrier et al. [2013] estimated erosion rates in 33 basins across Kauaʻi by measuring the mass of rock eroded from each basin over the basin's lifetime, an approach that yields erosion rates averaged over the area of the drainage basin and over the duration of erosion. These Myr-scale basin-averaged erosion rates range from 8 t km^{-2} yr^{-1} to 335 t km^{-2} yr^{-1} across Kaua'i and are positively correlated with modern basin-averaged mean annual precipitation rates (Figure 5). There is a large difference in timescale between the modern precipitation rates in Figure 5 and the paleoprecipitation rates that helped shape Kaua'i's topography over the past 5 Myr, as there is in any study that links long-term landscape evolution to modern climate measurements. However, even though Kaua'i's paleoclimatic history is poorly constrained [e.g., *Hotchkiss et al.*, 2000], asymmetries in pyroclastic cones suggest that the dominant direction of the trade winds were similar during glacial and interglacial periods [*Porter*, 1997], which suggests that spatial patterns in paleoprecipitation may have been similar to those today, even if the magnitudes of paleoprecipitation rates are not well known. Furthermore, there are no obvious geological controls across Kaua'i that would generate the observed correlation between erosion rates and modern precipitation rates in Figure 5. Thus, the observations in Figure 5 are consistent with a positive influence of rainfall rates on long-term erosion rates, and are consistent with the notion that spatial patterns in rainfall steer the topographic development of volcanic islands.

Several studies have taken advantage of steep intra-island rainfall gradients to show that rates of soil development in Hawaii are mediated by climate. *Chadwick et al.* [2003], for instance, examined soil profiles at sixteen sites on Hawaii's Kohala peninsula, across which mean annual precipitation ranged from 0.16 m yr^{-1} to 3 m yr^{-1}. They observed that soils at sites with high mean annual precipitation rates have higher concentrations of noncrystalline material and lower concentrations of crystalline minerals and base cations than soils in dry areas. Along three rainfall gradients on Hawaii, *Porder et al.* [2007] measured the enrichment of presumably immobile Nb in soil relative to its parent rock and concluded that soil chemical mass losses are 3-8 times higher at sites where mean annual precipitation rates exceed 1-1.5 m yr^{-1} than at drier sites.

On San Cristobal Island in the Galápagos, there is a strong association between elevation, rainfall, and soil development and hydraulic properties. Above 350 m elevation, where precipitation is about 2 m yr^{-1}, soils have substantial accumulations of clay minerals, relatively low porosity (<25%), and relatively low permeability (10^{-12} to 10^{-13} m^2). At lower elevations, rainfall is about 0.5 m yr^{-1}, and soils have developed primarily from mechanical alteration, and therefore have few clay minerals. In these low elevation soils, porosity is relatively high (35-40%), as is permeability (10^{-10} to 10^{-11} m^2) [*Adelinet et al.*, 2008]. As with the observations in Hawaii, these climosequence studies show that soils weather and develop clay-rich, low-permeability horizons more quickly in wetter places. Because not all of these climosequence studies quantified soil production rates, a comparison of the extent of soil chemical weathering at these sites cannot distinguish between the effects of mineral supply rates and those of climate [*Riebe et al.*, 2004; *Yoo and Mudd*, 2008]. Nonetheless, these observations of soils in the Galapagos as well as those in Hawaii are consistent with faster chemical weathering and faster development of clay-rich, low permeability horizons in wetter soils. Thus, to the extent that high rainfall rates accelerate the development of low-permeability soils, high rainfall rates should also lead more quickly to less groundwater recharge and more surface runoff.

The seasonal distribution and intensity of rainfall may be an important control on the patterns and timescales of landscape evolution of volcanoes, because higher intensity rainfall can result in more efficient erosion than lower intensity rainfall, even if mean annual precipitation rates are the same [e.g., *Molnar*, 2001; *Lague et al.*, 2005; *Molnar et al.*, 2006; *Wu et al.*, 2006]. A compilation of World Meteorological Organization (WMO) records shows strong differences in the seasonality of precipitation among ocean islands (Table 2). Because these data are monthly, they may mask even more dramatic differences in event-scale rainfall intensity across regions. The low elevation bias of the WMO stations may also obscure contributions of cloud water interception (fog drip) to the water budget, which can be significant at higher elevations in some regions [*Scholl et al.*, 2002; *Prada et al.*, 2009; *Pryet et al.*, 2012].

Field observations suggest that high-intensity rainfall, like that in the Cape Verde, Azores, and Canary Islands, drives faster landscape dissection than gentle, low-intensity precipitation and cloud water interception, such as typically occurs in the Galápagos Islands. The comparison between Cape Verde and the Galápagos is not perfect, because styles of volcanism and resulting volcanic products and architecture are different [*McBirney and Williams*, 1969; *Ramalho*, 2011], but it does illustrate the role of precipitation intensity in affecting rates of landscape evolution.

The Cape Verde Archipelago's arid climate is governed by seasonal shifts of the Inter Tropical Convergence Zone and the Azores anticyclone, causing an extremely variable rainfall regime [*Mannaerts and Gabriels*, 2000]. During the months of July-

October, the area experiences a southwesterly monsoon – “the wet season”, accounting for almost 80% of the annual precipitation – whereas during the rest of the year, dry northeast trade winds prevail and virtually no precipitation occurs [*Vailleux and Bourgue*, 1974; *Mannaerts and Gabriels*, 2000; *Heilweil et al.*, 2009]. Even during the wet season, most rain falls in just a few days [*Heilweil et al.*, 2009]. Local rainfall is strongly dependent on elevation, with some low coastal areas having no rainfall or fog condensation for several years at a time. Coastal areas average 0-150 mm yr^{-1} of rain, in contrast to 800-1000 mm yr^{-1} in the mountain areas above 1000 m a.m.s.l. [*Vailleux and Bourgue*, 1974; *Langworthy and Finan*, 1997; *Mannaerts and Gabriels*, 2000; *Heilweil et al.*, 2009]. When rainstorms occur, precipitation is intense [*Da Rocha Faria*, 1971], and an annual maximum 24 hour storm may represent an average of 45% of total annual rainfall [*Mannaerts and Gabriels*, 2000]. Streams are ephemeral but torrential.

The strong erosivity of the Cape Verde precipitation regime is evident in the morphology of Fogo Island. The island is probably entirely Quaternary [*Brum da Silveira et al.*, 1995], and the Pico do Fogo stratocone, which is built in an old caldera/flank collapse scar, is Holocene with numerous historical eruptions [*Brum da Silveira et al.*, 1995]. Despite its young age, Pico do Fogo already exhibits erosional gullies, carved in the loose scoria and scree that constitute the cone’s upper slope. Likewise, in the surrounding landscape of historical cones and flows, incipient gullies have started to form on the sides of the lava flows, the depressions between flows, or within lower channels of the flows. There is evidence for water runoff in some of the emptied lava channels, bounded by levees, which have smoother, less permeable surfaces, bounded by levees. In the lower areas, gullies develop preferentially where the substratum is composed of older, fine distal pyroclastic deposits, which are less permeable than the porous lava flows.

In contrast to Cape Verde, rainfall in the Galápagos is usually low intensity, although it too is strongly influenced by orography. Annual precipitation varies from <300 mm at the coast to >1600 mm at the summit of Santa Cruz Island, for which the climate records are most extensive. More than 80% of cool season days with recorded precipitation produced <2 mm of rain at low elevations. Higher elevations also have low intensity rainfall, with a significant fraction of the total precipitated water resulting from fog condensation in the forest canopy [*Trueman and d'Ozouville*, 2010]. All cool season precipitation can be infiltrated in low elevation zones, which have extremely high hydraulic conductivity (3600 mm/hr). At higher elevations, the infiltration capacity is lower, but still relatively high (3.6 mm/hr) [*Adelinet et al.*, 2008], and there is greater vegetative water demand than at low elevations. Thus, the cool season precipitation regime is unable to generate significant runoff that would enable erosion.

During the hot season, Galápagos rainfall can be more intense and spatially localized than during the cold season, and there is more potential for runoff generation and erosion. Over 40% of hot season rain days produced >5 mm of precipitation, and 10 days in a 40 year period generated >100 mm of rainfall near sea level at the Charles Darwin Foundation station on Santa Cruz. At the Bella Vista station on Santa Cruz, which at 194 m above sea level is the best available dataset for higher elevation locations, as much as 490 mm has occurred in a single day of hot season rainfall [*Trueman and d'Ozouville*, 2010]. At low elevations, infiltration capacity is greater than hot season rainfall intensity, so there is unlikely to be any significant runoff generation in the coastal zone. At higher elevations, rainfall rates can exceed the infiltration capacity or produce saturated soils and result in runoff. The potential for runoff generation is evidenced by ephemeral channels on the south side of Santa Cruz Island at elevations above 150 m [*d'Ozouville et al.*, 2008]. These channels are generally <10 m wide and a few meters deep or even shallower. Below 150 m elevation, the channels virtually disappear, either because they lose water to the underlying fractured basalt or because sediment loads become higher than the carrying capacity of the discharge [*d'Ozouville et al.*, 2008]. Except for San Cristóbal, the other Galápagos shields have even less evidence of runoff-driven erosion than Santa Cruz. It appears that the generally low intensity precipitation limits the efficacy of fluvial erosion throughout the Galápagos Islands.

The rates and spatial patterns of soil development and valley incision on the Hawaiian, Cape Verde, and Galápagos islands strongly covary with rainfall rates at both the annual and event timescales. If this is generally true of volcanic islands, it implies that spatial patterns in climate may strongly influence spatial patterns of hydrologic and topographic evolution. The comparison between the Cape Verde and Galápagos also highlights the need for more data on short-term and long-term erosion rates in both landscapes. Future work on the effects of precipitation rate on erosion and soil development could focus on linking the distribution of water flow between the surface and subsurface to weathering states and rates, erosion rates, and the spatial distribution of precipitation. Future work could also focus on quantifying the role of precipitation variability and intensity, and resultant soil moisture variability, on chemical weathering processes and fluxes, especially in semi-arid and arid volcanic landscapes. Finally, the potential importance of precipitation variability in driving dissection highlights the need for a better understanding of past precipitation regimes, and the role of paleoclimates in shaping modern volcanic landscapes.

4D. Flank collapses can hasten topographic dissection

Flank collapses of volcanic ocean islands are among the largest landslides on Earth [*Moore et al.*, 1989] and produce major, almost instantaneous topographic change. They are linked to hydrology through the possible triggering mechanisms of the slope failures and their after-effects on hydrology and topographic evolution. These massive landslides – which we distinguish from the small (~10-1000 m^2 in area), shallow (up to several meters thick), soil-based landslides common in island interiors [e.g., *Scott and Street*, 1976] – can set hydrologic and geomorphic evolution on a new trajectory by steepening slopes, creating knickpoints that drive fluvial incision, and short-circuiting groundwater flowpaths. Flank collapses have been documented on numerous ocean islands, including in the Cape Verde [*Madeira et al.*, 2008], Galápagos [*Naumann and Geist*, 2000; *Geist et al.*, 2002], and Hawaiian Islands [*Moore et al.*, 1989; *Presley et al.*, 1997; *Clague and Moore*, 2002; *Lamb et al.*, 2007].

Flank collapses may occur at any point in a volcano's development. The largest landslides tend to occur near the end of the shield-building stage, when the volcano reaches its maximum height, but they can continue to occur after eruptive activity has ceased [*Moore et al.*, 1989]. The shallow slope angles of shield volcanoes suggest that landslides may require some other trigger in addition to gravitational pull, but no widely accepted explanation for the causes or triggers of volcanic landslides currently exists [*Iverson*, 1995]. Steep submarine slopes and heights greater than 2500 m seem to predispose some ocean islands to landslides [*Mitchell*, 2003].

Groundwater could contribute to triggering landslides by reducing frictional resistance to failure through groundwater seepage or by inducing phreatomagmatic eruptions [*Violette et al.*, 2001]. The substantial groundwater slopes required for initiation of sliding are not commonly found in ocean island volcanoes, but thick low-permeability clay layers could enhance landslide potential [*Iverson*, 1995]. *Clague and Moore* [2002] speculate that phreatomagmatic eruptions could produce large lateral forces which contribute to slope failures and landsliding. These eruptions would be controlled by the availability of a groundwater reservoir that could be pressurized and converted to steam. *Clague and Dixon* [2000] suggest that the possibility of phreatomagmatic eruptions is correlated with high rainfall rates. Where rainfall rates are too low, volcanoes cannot maintain an active hydrothermal system, because water is converted to steam faster than groundwater is replenished [*Clague and Dixon*, 2000], thus limiting the potential for groundwater to be involved in landslide triggering. However, massive landslides have occurred on volcanoes with a wide range of precipitation rates [*Mitchell*, 2003], so the necessity of precipitation or groundwater as a triggering force is not clear.

On Kohala volcano on Hawai'i, a massive landslide, likely between 250 and 230 ka, created a scarp now expressed as cliffs up to 450 m high along a ~20 km section of coast. This section of Kohala is much more dramatically dissected than the area to the north of the slide, where rainfall and bedrock geology are comparable. Valleys draining towards the landslide scarp are 350-750 m deep and abruptly terminate in an amphitheater shape [*Lamb et al.*, 2007]. This distinct valley morphology, coupled with observation of springs along valley walls, prompted several authors to suggest that these valleys were formed by groundwater seepage erosion [*Kochel and Piper*, 1986; *Baker and Gulick*, 1987]. However, there is little evidence that seepage erosion is capable of forming valleys in basalt [*Lamb et al.*, 2006], and more recent interpretation has focused on the role of the landslide in creating a knickpoint that has propagated upstream via plunge pool erosion and undercutting at the base of waterfalls [*Lamb et al.*, 2007]. This interpretation requires that landscape evolution on Kohala proceeded to the extent that streams carried sufficient water and sediment to cause knickpoint retreat and valley erosion, either before the landslide or sufficiently soon after the landslide to produce the valleys observed today. The existence of numerous smaller, perched fluvial valleys draining to the Kohala coast suggests that such fluvial incision could indeed have occurred.

While knickpoint retreat by waterfall erosion as a mechanism for landscape evolution following landsliding is compelling and may apply in many settings, *Llanes et al*. [2009] suggest that knickpoint retreat from a landslide scarp is observed in the absence of waterfalls on La Gomera in the Canaries. This setting is presently more arid than Hawaii and waterfalls are sparse or absent. Instead, *Llanes et al*. [2009] attribute retreat to seepage erosion at the contact between younger and older strata. Thus, there may be a climatic determinant influencing the way volcanic landscapes evolve following landslides, but volcanic architecture is also important. Because valleys take time to erode headward, the morphological extent of the failure is also affected by the time since flank collapse. For example, the massive landslide scarp on Ta'u in American Samoa is only weakly dissected, which may reflect the short time since the failure occurred (<70 ka) [*McDougall*, 2010].

It is clear that, where they occur, flank collapses have a profound influence on the subsequent evolution of volcanic landscapes by hastening dissection and perhaps by shifting patterns of volcanism. One estimate suggests that the rate of mass removal by flank collapses may be equivalent to that accomplished by fluvial erosion [*Madeira et al.*, 2008]. More such comparisons, across a range of climates and tectonic settings, would help constrain the global and geologic role of landsliding in shaping volcanic evolution. As described above, much remains to be determined about the role of groundwater in triggering volcanic landslides and the mechanisms by which they promote dissection or volcanic rejuvenation.

4E. Volcanic architecture and tectonics constrain the patterns of landscape evolution

In addition to the climatic factors described in preceding sections, there is an underlying set of geologic and tectonic properties that constrain the evolution of volcanic landscapes. Volcanic architecture, including rock properties and stratigraphy, controls the initial distribution of water between the surface and subsurface and the distribution of hydrologic flowpaths within the subsurface. This initial template may continue to affect the trajectory of landscape evolution throughout its development, while the tectonic setting controls the base level to which hydrologic and geomorphic processes must adjust.

An ocean island generally goes through a sequence of constructional stages that form its architecture. The transition between seamount and emergent island is typically characterized by highly explosive hydrovolcanism, followed by effusive activity that builds a large lava shield. Later, towards the end of the shield-building stage, volcanism becomes more explosive, producing brecciated deposits and collapse calderas. Intensive hydrothermal alteration may occur during this time. This period is often followed by one of quiescence, but rejuvenation of the volcano may occur, generating a second shield building phase or more frequently one or more low-volume post-erosional volcanic stages [*Peterson and Moore*, 1987]. This sequence leads to complex subsurface architecture that exerts strong controls on hydrologic flowpaths. Even in shield volcanoes and ocean islands with less complex geologic histories, volcanic architecture can substantially influence hydrologic and landscape evolution.

There are two dominant conceptual models for groundwater flow in shield and ocean island volcanoes. In one model, a basal aquifer exists near sea level and higher elevation groundwater is either perched on impermeable layers or impounded by dikes. Dikes and sills tend to be low-permeability barriers to groundwater flow, but if they are extensively fractured with little mineral infilling of the fractures, they can act as zones of preferential flow [*Custodio*, 2007]. This perched and dike-impounded model was developed to explain hydrogeologic features of Hawaiian volcanoes [*Stearns*, 1942; *Izuka and Gingerich*, 2003], and may be appropriate for the Galápagos [*d'Ozouville et al.*, 2008; *Pryet et al.*, 2012], Cape Verde [*Heilweil et al.*, 2009] and Piton de la Fournaise [*Violette et al.*, 1997]. An alternative model assumes that permeability decreases with depth as a result of compaction and hydrothermal alteration [*Custodio*, 1989; 2007]. Decreasing permeability with depth would mean that near surface volcanic deposits are the most important hydrogeologically, with a water table that forms a dome across the volcano, as a subdued mirror of surface topography. In this case, high elevation groundwater could be connected to basal groundwater near sea level on ocean islands, as appears to be the case on Piton des Neiges and in the Canary Islands [*Custodio*, 1989; *Join et al.*, 2005]. In the Cape Verde Islands, strong permeability contrasts exist between shield-stage and underlying basement complexes, with springs emerging along the contact. Declining permeability with depth is also likely the appropriate conceptual model for the hydrogeology of the Oregon Cascades [*Saar and Manga*, 2004; *Jefferson et al.*, 2006].

The implications of these two conceptual models for hydrologic and topographic evolution need to be explored.

The style and products of a volcanic eruption, specifically the permeability and consolidation of the deposit, can strongly affect hydrologic and geomorphic processes and rates following emplacement, by controlling the initial infiltration capacity and erodibility of the landscape. In general, subaerial basalt lavas are much more permeable (10^{-9} to 10^{-15} m^2) and more consolidated than more explosive volcanic products (10^{-12} to 10^{-21} m^2). The permeability of basaltic lava flows is also strongly anisotropic, with permeability parallel to the flow surface typically 2 to 100 times greater than surface-normal permeability [*Singhal and Gupta*, 2010]. In pahoehoe flows, permeability is primarily the result of lava tubes and gas vesicles, whereas in a'a flows, autobrecciated top and bottom surfaces are the major zone of permeability. Interflow spaces may also be high permeability zones, and with basalt flows typically 1-6 m thick, a vertical section encompasses many such zones [*Davis*, 1969; *Kilburn*, 2000]. Spring and channel locations appear to be influenced by lava flow geometry [*Jefferson et al.*, 2006; *Jefferson et al.*, 2010], and the mechanisms by which lava morphology controls spring occurrence and incipient channel development is an area where more research is needed. For hyaloclastite, permeability is strongly affected by the extent of secondary alteration [*Frolova*, 2010], and for ocean islands with steeper slopes and more explosive histories, lahar and tuff deposits may contribute to runoff generation and dissection. [*Lavigne et al.*, 2000]. In tuffs, permeability is controlled by the abundance of phenocrysts and rock fragments and the extent of welding and compaction [*Smyth and Sharp*, 2006].

Even from a single volcano, multiple eruptive styles can produce a highly heterogeneous landscape. Far from the volcanic vent, lava flows may be interbedded with sediment, fine ash, and soil. Closer to volcanic vents, pyroclastic materials may dominate the section [*Custodio*, 2007]. Groundwater patterns reflect the three-dimensional spatial variability of eruptive products, as evidenced by the correspondence between well yields and lithology on Jeju Island [*Won et al.*, 2005]. On Santa Cruz and San Cristóbal in the Galápagos, the presence of perched aquifers may be attributed to a low permeability layer formed from weathered ash or colluvial material that was baked by subsequent lava flows [*d'Ozouville et al.*, 2008; *Pryet et al.*, 2012].

A volcanic island's landscape evolution is also affected by the island's tectonic setting. Unlike many continental mountain ranges, volcanic islands are generally not in topographic steady state. That is, erosion rates on volcanic islands are rarely offset by rock uplift rates, unlike in steady-state landscapes (Figure 6). Instead, vertical motion rates on volcanic islands are generally negative: islands subside. Island subsidence is driven by a number of processes, including isostatic adjustment of the oceanic lithosphere, which progresses faster under larger or faster-growing islands; changes in dynamic topography as an island migrates away from a hotspot's topographic swell; and continued cooling and contraction of the volcano [e.g., *Zhong and Watts*, 2002]. Although some islands experience short periods of uplift – Oahu, for example, currently appears to be rising on the flexural bulge created by Hawaii's growing load [*Grigg and Jones*, 1997; *Grigg*, 1998] – such hiatuses in subsidence are usually temporary. The dominant topographic history for a post-constructional volcanic island is a coordinated effort by fluvial and marine erosion and subsidence to bring the island down to sea level.

The 2-6 Ma Cape Verde islands illustrate the importance of tectonics on spatial patterns of dissection. In contrast to most other ocean islands, most of the Cape Verde Islands have been vertically stable over their lifetime or have experienced uplift [*Madeira et al.*, 2010; *Ramalho et al.*, 2010c; b; *Ramalho et al.*, 2010a] and their morphology reflects a competition between uplift and erosion. This competition is seen most starkly in some of the old (15-26 Ma) island volcanoes, which were completely or partially razed by marine erosion during the Plio-Quaternary, and then exposed again by recent uplift [*Ramalho et al.*, 2010c; *Ramalho et al.*, 2010a; *Ramalho*, 2011]. This razed morphology is interrupted only by residual isolated hills that escaped marine erosion and young volcanic cones of the last post-erosional stage [*Ramalho et al.*, 2010c; *Ramalho et al.*, 2010a; *Ramalho*, 2011]. The islands generally have a central region that is elevated but deeply dissected, surrounded by concentric rings of marine terraces with very low gradients in the seaward direction [*Ramalho*, 2011]. The present day drainage network is thus incipient when dissecting the razed morphology exposed by uplift, and it is highly evolved when dissecting old elevated areas. Incision is enhanced when streams reach the inner, highly impermeable basement complexes (typically uplifted, hydrothermally altered, submarine volcanic units) [*Serralheiro*, 1976; *Ramalho et al.*, 2010c]. Large alluvial fans radiate from deep canyons that dissect the central elevated region, covering adjacent razed flatlands with flood deposits. In effusive valley-filling lavas and associated coastal lava-deltas, second and third generation valleys, recurrently superimposed on each other by lava filling processes and subsequent fluvial erosion, are not uncommon. Overland flow and soil wash are enhanced by the low permeability of the old lithologies, leading to a barren and dusty landscape [*Ramalho*, 2011].

The examples of the Hawaiian and Cape Verde Islands suggest that there are many open research questions about how volcanic landscape evolution depends on tectonic history and internal volcanic architecture. These are challenging questions because uplift and subsidence patterns may vary in space and time, even within the same regional tectonic setting, and because hydrologic flowpaths can be strongly influenced by complexities in a volcano's three-dimensional architecture.

5. Other controls on volcanic landscape evolution

In addition to the factors described in Section 4, there are several other factors that may affect volcanic landscape evolution that we have not discussed for the sake of brevity or due to the relative scarcity of previous research to review. Here we list two additional factors that may be particularly important drivers of hydrologic and geomorphic evolution in certain geographic regions: glaciation and biota.

In temperate and polar latitudes, glaciation may shape landscape evolution much more dramatically than riverine processes. For example, the glaciated volcanoes of the Oregon Cascades stand out as the only volcanoes <500 ka that were substantially dissected in our data compilation (Figure 2). In a few other locations, there are shield volcanoes and ocean islands strongly influenced by past or present glaciation. These include Iceland [*Andrew and Gudmundsson*, 2007; *Jakobsson and Gudmundsson*, 2008], Antarctica and sub-Antarctic Islands [*McDougall et al.*, 2001; *Smellie et al.*, 2006], and the Northern Cordillera Volcanic Province of North America [*Edwards et al.*, 2011].

Life is also clearly one of the factors that mediates hydrologic and topographic changes as volcanic landscapes evolve, but the effects of microbial, plant, and animal communities are not understood well enough to make a definitive statement about whether the different ecological settings that exist on shield volcanoes and ocean islands lead to different trajectories of hydrologic and geomorphic evolution. This is clearly a promising area for future research. For example, there may prove to be detectable differences in landscape evolution between islands with similar climates but different degrees of biogeographical isolation. On the other hand, it is also possible that even very different microbial and plant communities can fill the same ecological niches and play the same roles in weathering soil development, and hydrology on different volcanoes, such that landscape evolution is still ultimately controlled by hydrologic processes.

6. Conclusions

Volcanic ocean islands and shield volcanoes are excellent natural laboratories in which to investigate the processes by which hydrology and topography co-evolve. Based on an analysis of 97 shield and ocean island volcanoes, we suggest that substantial dissection of volcanic landscapes typically begins between 0.5 and 2 Myr after eruption of the lavas that form the main shield. This apparent lag between construction and dissection may reflect the time necessary for processes of soil development and dust deposition to produce hydrological changes essential to generate sufficient erodible material and streamflow for dissection to proceed.

This compilation also reveals that topographic dissection tends to begin earlier on islands with higher mean annual precipitation. This lends empirical support to the expectation that water should drive the topographic and hydrologic evolution of volcanic islands. It is clear, however, that mean annual precipitation alone is an inadequate proxy for the many ways that water mediates volcanic landscape evolution. For instance, river incision rates may depend more on fluctuations in precipitation rates than on mean annual precipitation; soil development and dust deposition may occur at rates that are not proportional to mean annual precipitation; chemical and physical erosion rates change over time and may depend on precipitation rates in different ways; and flank collapses may be more likely to be triggered by rare, large storms than by average rainfall. In addition to such climatic effects, volcanic architecture and regional tectonics set the initial template for hydrology and topography, and likely constrain the possible trajectories for hydrologic and geomorphic evolution. All of these issues are candidate subjects for future research. To better understand the evolution of volcanic ocean islands and shield volcanoes, we suggest that efforts should be directed toward integrating a three-dimensional geologic perspective of volcanic architecture and tectonics with a stronger understanding of the ways in which precipitation-driven processes mediate the topographic evolution of landscapes undergoing remarkable permeability changes.

Acknowledgements

We are grateful to the organizing committee of the Chapman conference on The Galápagos As a Laboratory for the Earth Sciences for the invitation to participate in the conference and to the monograph editors for their tireless work. We also thank Noémi d'Ozouville, Gordon Grant, Natalia Deligne, Bill Dietrich, Leif Karlstrom, and others for useful conversations about volcanic landscape evolution and hydrology, and Sophie Violette and Josh Roering for constructive reviews. R. Ramalho's work is funded by DFG – The German Research Foundation.

References Cited

Adelinet, M., J. Fortin, N. D'Ozouville, and S. Violette (2008), The relationship between hydrodynamic properties and weathering of soils derived from volcanic rocks, Galápagos Islands (Ecuador), *Environ. Geol.*, *56*(1), 45-58.

Andrew, R. E. B., and A. Gudmundsson (2007), Distribution, structure, and formation of Holocene lava shields in Iceland, *J. Volcanol. Geotherm. Res.*, *168*(1-4), 137-154.

Baker, V. R., and V. C. Gulick (1987), Valley development on Hawaiian volcanoes *Tech. Memo. 89810*, 297-299 pp, Natl. Aeronaut. Space Admin., Washington, D.C.

Bard, E., B. Hamelin, M. Arnold, L. F. Montaggioni, G. Cabioch, G. Faure, and F. Rougerie (1996), Deglacial sea-level record from Tahiti corals and the timing of global meltwater discharge, *Nature*, *382*(6588), 241-244.

Benedeti, M. F., et al. (2003), Chemical weathering of basaltic lava flows undergoing extreme climatic conditions: the water geochemistry record, *Chem. Geol.*, *201*, 1-17.

Berner, R. A., and M. F. Cochran (1998), Plant-induced weathering of Hawaiian basalts, *J. Sedimentary Res.*, *68*(5), 723-726.

Brimhall, G. H., C. J. Lewis, J. J. Ague, W. E. Dietrich, J. Hampel, T. Teague, and P. Rix (1988), Metal enrichment in bauxites by deposition of chemically mature aeolian dust, *Nature*, *333*, 819-824.

Brum da Silveira, A., A. Serralheiro, I. Martins, J. Cruz, J. Madeira, J. Munhé, J. Pena, L. Matias, and M. L. Senos (1995), A erupção da Chã das Caldeiras, Ilha do Fogo de 2 de Abril de 1995, *Protecção Civil*, *7*, 3-14.

Carreira, P. M., J. M. Marques, A. Pina, A. M. Gomes, P. A. G. Fernandes, and F. M. Santos (2010), Groundwater Assessment at Santiago Island (Cabo Verde): A Multidisciplinary Approach to a Recurring Source of Water Supply, *Water Resour. Management*, *24*(6), 1139-1159.

Chadwick, O. A., L. A. Derry, P. M. Vitousek, B. J. Huebert, and L. O. Hedin (1999), Changing sources of nutrients during four millions years of ecosystem development, *Nature*, *397*, 491-497.

Chadwick, O. A., R. T. Gavenda, E. F. Kelly, K. Ziegler, C. G. Olson, W. C. Elliot, and D. M. Hendricks (2003), The impact of climate on the biogeochemical functioning of volcanic soils, *Chem. Geol.*, *292*, 195-223.

Clague, D. A., and J. E. Dixon (2000), Extrinsic controls on the evolution of Hawaiian ocean island volcanoes, *Geochem. Geophys. Geosyst.*, *1*(4), 1-9.

Clague, D. A., and J. G. Moore (2002), The proximal part of the giant submarine Wailau landslide, Molokai, Hawaii, *J. Volcanol. Geotherm. Res.*, *113*(1–2), 259-287.

Cruz, J., R. Coutinho, D. Pacheco, R. Cymbron, P. Antunes, P. Freire, and S. Mendes (2011), Groundwater salinization in the Azores archipelago (Portugal), *Environ. Earth Sci.*, *62*(6), 1273-1285.

Custodio, E. (1989), Groundwater characteristics and problems in volcanic rock terrains, in *Isotope Techniques in the Study of the Hydrology of Fractured and Fissured Rocks*, edited, pp. 87-137, IAEA, Vienna.

Custodio, E. (2007), Groundwater in volcanic hard rocks, in *Groundwater in Fractured Rocks*, edited by J. Krásný and J. M. Sharp, pp. 95-105, Taylor and Francis.

d'Ozouville, N., E. Auken, K. Sorensen, S. Violette, G. de Marsily, B. Deffontaines, and G. Merlen (2008), Extensive perched aquifer and structural implications revealed by 3D resistivity mapping in a Galápagos volcano, *Earth Planet. Sci. Lett.*, *269*(3-4), 517-521.

Da Rocha Faria, J. M. (1971), Frequency analysis of the annual highest values of the daily precipitation in some Portuguese overseas sites, *Fomento (Lisbon)*, *9*(3), 237-270.

Daly, C., R. P. Nielson, and D. L. Phillips (1994), A statistical-topographic model for mapping climatological precipitation over mountanious terrain, *Journal of Applied Meteorology*, *33*, 140-158.

Daly, C., W. P. Gibson, G. H. Taylor, G. L. Johnson, and P. Pasteris (2002), A knowledge-based approach to the statistical mapping of climate, *Climate Research*, *22*, 99-113.

Davis, S. N. (1969), Porosity and permeability of natural materials, in *Flow Through Porous Media*, edited by R. J. M. De Wiest, pp. 53-89, Academic Press, New York.

Deligne, N. I. (2012), After the Flow: Landscape Response to the Emplacement of Holocene Lava Flows, Central Oregon Cascades, USA, 237 pp, University of Oregon, Eugene, Ore.

Deligne, N. I., K. V. Cashman, and J. J. Roering (2012), After the lava flow: The importance of external soil sources for plant colonization of recent lava flows in the central Oregon Cascades, USA, *Geomorphol.*

Dohrenwend, J. C., A. D. Abrahams, and B. D. Turrin (1987), Drainage development on basaltic lava flows, Cima volcanic field, southeast California and Lunar Crater volcanic field, south-central Nevada, *Geol. Soc. Am. Bull.*, *99*, 405-413.

Doty, R. D., H. B. Wood, and R. A. Merriam (1981), Suspended sediment production from forested watersheds on Oahu, Hawaii, *J. Am. Water Resour. Assoc.*, *17*(3), 399-404.

Dunne, T., and L. B. Leopold (1978), *Water in Environmental Planning*, 818 pp., W.H. Freeman, San Francisco.

Edwards, B. R., J. K. Russell, and K. Simpson (2011), Volcanology and petrology of Mathews Tuya, northern British Columbia, Canada: glaciovolcanic constraints on interpretations of the 0.730 Ma Cordilleran paleoclimate, *Bull. Volcanol.*, *73*(5), 479-496.

Engels, M. S., C. H. I. Fletcher, M. E. Field, C. D. Storlazzi, E. E. Grossman, J. J. B. Rooney, C. L. Conger, and C. Glenn (2004), Holocene reef accretion: southwest Molokai, Hawaii, USA, *J. Sedimentary Res.*, *74*(2), 255-269.

Eppes, M. C., and J. B. J. Harrison (1999), Spatial variabilty of soils developing on basalt flows in the Potrillo Volcanic Field, southern New Mexico: prelude to a chronosequence study, *Earth Surf. Proc. Land.*, *24*, 1009-1024.

Ferrier, K. L., and J. W. Kirchner (2008), Effects of physical erosion on chemical denudation rates: A numerical modeling study of soil-mantled hillslopes, *Earth Planet. Sci. Lett.*, *272*, 591-599.

Ferrier, K. L., J. T. Perron, S. Mukhopadhyay, M. Rosener, J. D. Stock, K. L. Huppert, and M. Slosberg (2013), Covariation of climate and long-term erosion rates across a steep rainfall gradient on the Hawaiian island of Kaua'i, *Geol. Soc. Am. Bulletin*.

Fisher, R. V. (1995), Decoupling of pyroclastic currents: hazards assessments, *J. Volcanol. Geotherm. Res.*, *66*, 257-263.

Frolova, Y. (2010), Patterns of transformations in the compositions and properties of Icelandic hyaloclastites during lithogenesis, *Moscow Univ. Geol. Bull.*, *65*(2), 104-114.

Geist, D. J., W. M. White, F. Albarede, K. Harpp, R. Reynolds, J. Blichert-Toft, and M. D. Kurz (2002), Volcanic evolution in the Galapagos: The dissected shield of Volcan Ecuador, *Geochem. Geophys. Geosyst.*, *3*(10), 1061.

Gislason, S. R., S. Arnorsson, and H. Armannsson (1996), Chemical weathering of basalt in southwest Iceland: effects of runoff, age of rocks, and vegetative/glacial cover, *Am. J. Sci.*, *296*, 837-907.

Gleeson, T., L. Smith, N. Moosdorf, J. Hartmann, H. H. Durr, A. H. Manning, L. P. H. van Beek, and A. M. Jellinek (2011), Mapping permeability over the surface of the Earth, *Geophys. Res. Lett.*, *38*, LO2401, doi:2410.1029/2010GL045565

Grigg, R. W. (1998), Holocene coral reef accretion in Hawaii: a function of wave exposure and sea level history, *Coral Reefs*, *17*(3), 263-272.

Grigg, R. W., and A. T. Jones (1997), Uplift caused by lithospheric flexure in the Hawaiian Archipelago as revealed by elevated coral deposits, *Mar. Geol.*, *141*(1), 11-25.

Heilweil, V. M., D. K. Solomon, S. B. Gingerich, and I. M. Verstraeten (2009), Oxygen, hydrogen, and helium isotopes for investigating groundwater systems of the Cape Verde Islands, West Africa, *Hydrogeol. J.*, *17*(5), 1157-1174.

Heimsath, A. M., W. E. Dietrich, K. Nishiizumi, and R. C. Finkel (1997), The soil production function and landscape equilibrium, *Nature*, *388*(6640), 358-361.

Herrera, C., and E. Custodio (2008), Conceptual hydrogeological model of volcanic Easter Island (Chile) after chemical and isotopic surveys, *Hydrogeol. J.*, *16*(7), 1329-1348.

Hildenbrand, A., P. Y. Gillot, and C. Marlin (2008), Geomorphological study of long-term erosion on a tropical volcanic ocean island: Tahiti-Nui (French Polynesia), *Geomorphol.*, *93*(3-4), 460-481.

Hill, B. R., C. C. Fuller, and E. H. DeCarlo (1997), Hillslope soil erosion estimated from aerosol concentrations, North Halawa Valley, Oahu, Hawaii, *Geomorphol.*, *20*(1), 67-79.

Hotchkiss, S., P. M. Vitousek, O. A. Chadwick, and J. Price (2000), Climate cycles, geomorphological change, and the interpretation of soil and ecosystem development, *Ecosystems*, *3*, 522-533.

Inbar, M. (1994), The geomorphological evolution of the Paricutin cone and lava flows, Mexico, 1943-1990, *Geomorphol.*, *9*, 57-76.

Inbar, M., C. Risso, and C. Parica (1995), The morphological development of a young lava flow in the South Western Andes -- Neuquen, Argentina, *Z. Geomorphol.*, *39*(4), 479-484.

Ingebritsen, S. E., D. R. Sherrod, and R. H. Mariner (1992), Rates and patterns of groundwater flow in the Cascade Range volcanic arc, and the effect on subsurface temperatures, *Journal of Geophysical Research*, *97*, 4599-4627.

Iverson, R. M. (1995), Can magma-injection and groundwater forces cause massive landslides on Hawaiian volcanoes?, *J. Volcanol. Geotherm. Res.*, *66*(1-4), 295-308.

Izuka, S. K., and S. B. Gingerich (2003), A thick lens of fresh groundwater in the southern Lihue Basin, Kaua'i, Hawaii, USA, *Hydrogeol. J.*, *11*, 240-248.

Jakobsson, S. P., and M. T. Gudmundsson (2008), Subglacial and intraglacial volcanic formations in Iceland, *Jokull*, *58*, 179-196.

Jefferson, A., G. E. Grant, and T. P. Rose (2006), The influence of volcanic history on groundwater patterns on the west slope of the Oregon High Cascades, *Water Resour. Res.*, *42*, W12411, doi:12410.11029/12005WR004812.

Jefferson, A., G. Grant, S. Lewis, and S. Lancaster (2010), Coevolution of hydrology and topography on a basalt landscape in the Oregon Cascade Range, USA., *Earth Surf. Proc. Land.*, *35*(7), 803-816.

Join, J.-L., J.-L. Folio, and B. Robineau (2005), Aquifers and groundwater within active shield volcanoes. Evolution of conceptual models in the Piton de la Fournaise volcano, *J. Volcanol. Geotherm. Res.*, *147*(1-2), 187-201.

Kilburn, C. R. J. (2000), Lava flows and flow fields, in *Encyclopedia of Volcanoes*, edited by H. Sigurdsson, pp. 291-305, Academic Press, San Diego, Calif.

Kochel, R. C., and J. F. Piper (1986), Morphology of large valleys on Hawaii: evidence for groundwater sapping and comparisons with Martian valleys, *J. Geophys. Res.*, *91*(B13), E175-E192.

Koh, D. C., H. W. Chang, K. S. Lee, K. S. Ko, Y. Kim, and W. B. Park (2005), Hydrogeochemistry and environmental isotopes of ground water in Jeju volcanic island, Korea: implications for nitrate contamination, *Hydrol. Process.*, *19*(11), 2225-2245.

Kurtz, A. C., L. A. Derry, and O. A. Chadwick (2001), Accretion of Asian dust to Hawaiian soils: Isotopic, elemental, and mineral mass balances, *Geochim. Cosmochim. Acta*, *65*(12), 1971-1983.

Lague, D., N. Hovius, and P. Davy (2005), Discharge, discharge variability, and the bedrock channel profile, *J. Geophys. Res.*, *110*, F04006, doi:04010.01029/02004JF000259.

Lamb, M. P., A. D. Howard, W. E. Dietrich, and J. T. Perron (2007), Formation of amphitheater-headed valleys by waterfall erosion after large-scale slumping on Hawai'i, *Geol. Soc. Am. Bull.*, *119*(7/8), 805-822.

Lamb, M. P., A. D. Howard, J. Johnson, K. X. Whipple, W. E. Dietrich, and J. T. Perron (2006), Can springs cut canyons into rock?, *Journal of Geophysical Research*, *111*, E07002, doi:07010.01029/02005JE002663.

Langworthy, M., and T. J. Finan (1997), *Waiting for rain: agriculture and ecological imbalance in Cape Verde*, 212 pp., Rienner, Boulder, Colo.

Lavigne, F., J. C. Thouret, B. Voight, H. Suwa, and A. Sumaryono (2000), Lahars at Merapi volcano, Central Java: an overview, *J. Volcanol. Geotherm. Res.*, *100*, 423-456.

Li, Y. H. (1988), Denudation rates of the Hawaiian islands by rivers and groundwater, *Pacific Science*, *42*(3-4), 253-266.

Llanes, P., R. Herrera, M. Gomez, A. Munoz, J. Acosta, E. Uchupi, and D. Smith (2009), Geological evolution of the volcanic island La Gomera, Canary Islands, from analysis of its geomorphology, *Mar. Geol.*, *264*(3-4), 123-139.

Lohse, K. A., and W. E. Dietrich (2005), Contrasting effects of soil development on hydrological properties and flow paths, *Water Resour. Res.*, *41*, W12419, doi:12410.11029/12004WR003403.

Louvat, P., and C. J. Allegre (1997), Present denudation rates on the island of Reunion determined by river geochemistry: Basalt weathering and mass budget between chemical and mechanical erosions, *Geochim. Cosmochim. Acta*, *61*(17), 3645-3669.

Louvat, P., and C. J. Allegre (1998), Riverine erosion rates on Sao Miguel volcanic island, Azores archipelago, *Chem. Geol.*, *148*, 177-200.

Louvat, P., S. R. Gislason, and C. J. Allègre (2008), Chemical and mechanical erosion rates in Iceland as deduced from river dissolved and solid material, *American Journal of Science*, *308*(5), 679-726.

Ludwig, K. R., B. J. Szabo, J. G. Moore, and K. R. Simmons (1991), Crustal subsidence rate off Hawaii determined from $^{234}U/^{238}U$ ages of drowned coral reefs, *Geology*, *19*(2), 171-174.

Madeira, J., A. Brum da Silveira, J. Mata, C. Mourão, and S. Martins (2008), The role of mass movements on the geomorphologic evolution of island volcanoes: examples from Fogo and Brava in the Cape Verde archipelago, *Comunicações Geológicas*, *95*, 93-106.

Madeira, J., J. Mata, C. Mourao, A. B. da Silveira, S. Martins, R. Ramalho, and D. L. Hoffmann (2010), Volcano-stratigraphic and structural evolution of Brava Island (Cape Verde) based on Ar-40/Ar-39, U-Th and field constraints, *J. Volcanol. Geotherm. Res.*, *196*(3-4), 219-235.

Mannaerts, C., and D. Gabriels (2000), Rainfall erosivity in Cape Verde, *Soil and Tillage Res.*, *55*(3), 207-212.

Mastin, L. G., and J. B. Witter (2000), The hazards of eruptions through lakes and seawater, *J. Volcanol. Geotherm. Res.*, *97*(1-4), 195-214.

Matsuoka, I., M. Lum, and V. E. Kunishige (1992), Water Resources Data for Hawaii and Other Pacific Areas, Water Year 1991: Volume 1. Hawaii *HI-91-1*, 282 pp, U.S. Geol. Surv., Washington, D.C.

Matsuoka, I., G. A. Tateishi, M. Lum, and V. E. Kunishige (1991), Water Resources Data for Hawaii and Other Pacific Areas, Water Year 1990: Volume 1. Hawaii *HI-90-1*, 303 pp, U.S. Geol. Surv., Washington, D.C.

McBirney, A. R., and H. Williams (1969), *Geology and petrology of the Galápagos Islands*, 197 pp., Geol. Soc. Am., Boulder, Colo.

McDougall, I. (2010), Age of volcanism and its migration in the Samoa Islands, *Geol. Mag.*, *147*(5), 705-717.

McDougall, I., W. Verwoerd, and L. Chevallier (2001), K-Ar geochronology of Marion Island, Southern Ocean, *Geol. Mag.*, *138*(1), 1-17.

Menendez, I., P. G. Silva, M. Martin-Betancor, F. J. Perez-Torrado, H. Guillou, and S. Scaillet (2008), Fluvial dissection, isostatic uplift, and geomorphological evolution of volcanic islands (Gran Canaria, Canary Islands, Spain), *Geomorphol.*, *102*(1), 189-203.

Mitchell, N. C. (2003), Susceptibility of mid-ocean ridge volcanic islands and seamounts to large-scale landsliding, *J. Geophys. Res.*, *108*(B8), 34.

Molnar, P. (2001), Climate change, flooding in arid environments, and erosion rates, *Geology*, *29*(12), 1071-1074.

Molnar, P., R. S. Anderson, G. Kier, and J. Rose (2006), Relationships among probability distributions of stream discharges in floods, climate, bed load transport, and river incision, *J. Geophys. Res.*, *111*, F02001, doi:02010.01029/02005JF000310.

Montaggioni, L. F. (1988), Holocene reef growth history in mid-plate high volcanic islands, in *Proceedings of the 6th International Coral Reef Symposium: Vol. 3: Contributed Papers*, edited by J. H. Choat, et al., pp. 445-460, Townsville, Australia.

Montaggioni, L. F. (2005), History of Indo-Pacific coral reef systems since the last glaciation: development patterns and controlling factors, *Earth Sci. Rev.*, *71*(1), 1-75.

Montaggioni, L. F., G. Cabioch, G. F. Camoin, E. Bard, A. Ribaud Laurenti, G. Faure, P. Déjardin, and J. Récy (1997), Continuous record of reef growth over the past 14 k.y. on the mid-Pacific island of Tahiti, *Geology*, *25*(6), 555-558.

Moore, J. G., D. A. Clague, R. T. Holcomb, P. W. Lipman, W. R. Normank, and M. E. Torresan (1989), Prodigious submarine landslides on the Hawaiian Ridge, *J. Geophys. Res.*, *94*(B12), 17465-17484.

Nanzyo, M., S. Shoji, and R. Dahlgren (1993), Physical Characteristics of Volcanic Ash Soils, in *Volcanic Ash Soils - Genesis, Properties, and Utilization*, edited by S. Shoji, M. Nanzyo and R. Dahlgren, pp. 189-207, Elsevier, Amsterdam.

Naumann, T., and D. Geist (2000), Physical volcanology and structural development of Cerro Azul Volcano, Isabela Island, Galápagos: implications for the development of Galápagos-type shield volcanoes, *Bull. Volcanol.*, *61*(8), 497-514.

Németh, K., and S. J. Cronin (2011), Drivers of explosivity and elevated hazard in basaltic fissure eruptions: The 1913 eruption of Ambrym Volcano, Vanuatu (SW-Pacific), *J. Volcanol. Geotherm. Res.*, *201*(1-4), 194-209.

Peterson, D. W., and R. B. Moore (1987), Geologic history and evolution of geologic concepts, Island of Hawaii, in *Volcanism in Hawaii*, edited by R. W. Decker, T. L. Wright and P. H. Stauffer, pp. 149-189, U.S. Geological Survey Prof. Pap. 1350, Washington, D.C.

Pirazzoli, P. A., L. F. Montaggioni, G. Delibrias, G. Faure, and B. Salvat (1985), Late Holocene sea-level changes in the Society Islands and in the northwest Tuamotu atolls, in *The Fifth International Coral*, edited by C. Gabrie and J. L. Toffart, pp. 131-136, Tahiti.

Pokrovsky, O. S., J. Schott, D. I. Kudryavtzev, and B. Dupre (2005), Basalt weathering in Central Siberia under permafrost conditions, *Geochim. Cosmochim. Ac.*, *69*(24), 5659-5680.

Porder, S., G. E. Hilley, and O. A. Chadwick (2007), Chemical weathering, mass loss, and dust inputs across a climate by time matrix in the Hawaiian Islands, *Earth Planet. Sci. Lett.*, *258*, 414-427.

Porter, S. (1997), Late Pleistocene eolian sediments related to pyroclastic eruptions of Mauna Kea Volcano, Hawaii, *Quaternary Research*, *47*, 261-276.

Prada, S., M. M. de Sequeira, C. Figueira, and M. O. da Silva (2009), Fog precipitation and rainfall interception in the natural forests of Madeira Island (Portugal), *Agric. For. Meteorol.*, *149*(6-7), 1179-1187.

Presley, T. K., J. M. Sinton, and M. Pringle (1997), Postshield volcanism and catastrophic mass wasting of the Waianae Volcano, Oahu, Hawaii, *Bull. Volcanol.*, *58*(8), 597-616.

PRISM (2012), PRISM Climate Group, Oregon State University, in Secondary PRISM Climate Group, Oregon State University, http://prism.oregonstate.edu.

Pryet, A., C. Domínguez, P. F. Tomai, C. Chaumont, N. d'Ozouville, M. Villacís, and S. Violette (2012), Quantification of cloud water interception along the windward slope of Santa Cruz Island, Galapagos (Ecuador), *Agric. For. Meteorol.*, *161*, 94-106.

Rad, S. D., C. J. Allegre, and P. Louvat (2007), Hidden erosion on volcanic islands, *Earth Planet. Sci. Lett.*, *262*(1-2), 109-124.

Rad, S. D., K. Rive, and C. J. Allegre (2011), Weathering regime associated with subsurface circulation on volcanic islands, *Aquat. Geochem.*, *17*(3), 221-241.

Ramalho, R. (2011), *Building the Cape Verde Islands*, 262 pp., Springer.

Ramalho, R., G. Helffrich, D. N. Schmidt, and D. Vance (2010a), Tracers of uplift and subsidence in the Cape Verde archipelago, *J. Geol. Soc.*, *167*(3), 519-538.

Ramalho, R., G. Helffrich, M. Cosca, D. Vance, D. Hoffmann, and D. N. Schmidt (2010b), Episodic swell growth inferred from variable uplift of the Cape Verde hot spot islands, *Nature Geoscience*, *3*, 774-777.

Ramalho, R., G. Helffrich, M. Cosca, D. Vance, D. Hoffmann, and D. N. Schmidt (2010c), Vertical movements of ocean island volcanoes: Insights from a stationary plate environment, *Mar. Geol.*, *275*, 84-95.

Riebe, C. S., J. W. Kirchner, and R. C. Finkel (2004), Erosional and climatic effects on long-term chemical weathering rates in granitic landscapes spanning diverse climate regimes, *Earth Planet. Sci. Lett.*, *224*(3-4), 547-562.

Saar, M. O., and M. Manga (2004), Depth dependence of permeability in the Oregon Cascades inferred from hydrogeologic, thermal, seismic, and magmatic modeling constraints, *J. Geophys. Res.*, *109*(B4), B04204, 04210.01029/02003JB002855.

Scholl, M. A., S. B. Gingerich, and G. W. Tribble (2002), The influence of mictoclimates and fog on stable isotope signatures used in interpretation of regional hydrology: East Maui, Hawaii, *J. Hydrol.*, *264*, 170-184.

Schopka, H. H., and L. A. Derry (2012), Chemical weathering fluxes from volcanic islands and the importance of groundwater: The Hawaiian example, *Earth Planet. Sci. Lett.*, *339–340*(0), 67-78.

Scott, G. A. J., and J. M. Street (1976), The role of chemical weathering in the formation of Hawaiian amphitheatre-headed valleys., *Z. Geomorphol.*, *20*, 171-189.

Serralheiro, A. (1976), A Geologia da Ilha de Santiago (Cabo Verde), *Boletim do Museu e Laboratorio Mineralógico e Geológico da Faculdade de Ciências*, *14*, 157-369.

Singhal, B. B. S., and R. P. Gupta (2010), Hydrogeology of Volcanic Rocks, in *Applied Hydrogeology of Fractured Rocks*, edited, pp. 257-268, Springer Netherlands.

Slate, J. L., W. B. Bull, T.-L. Ku, M. Shafiqullah, D. J. Lynch, and Y.-P. Huang (1991), Soil-carbonate genesis in the Pinacate volcanic field, Northwestern Sonora, Mexico, *Quaternary Res.*, *35*(3, Part 1), 400-416.

Smellie, J. L., W. C. McIntosh, R. Esser, and P. Fretwell (2006), The Cape Purvis volcano, Dundee Island (northern Antarctic Peninsula): late Pleistocene age, eruptive processes and implications for a glacial palaeoenvironment, *Antarct. Sci.*, *18*(3), 399-408.

Smyth, R. C., and J. M. Sharp (2006), The hydrology of tuffs, in *Tuffs: Their Properties, Uses, Hydrology, and Resources*, edited by G. Heiken, pp. 91-112, Geological Society of America, Boulder, Co.

Stearns, H. T. (1942), Hydrology of volcanic terranes, in *Hydrology*, edited by O. E. Meinzer, pp. 678-703, McGraw-Hill, New York.

Stearns, H. T. (1946), Geology of the Hawaiian Islands *Bull. 8*, 106 pp, Territory of Hawaii Division of Hydrography, Hawaii.

Thouret, J. C. (1999), Volcanic geomorphology - an overview, *Earth-Sci. Rev.*, *47*(1-2), 95-131.

Trueman, M., and N. d'Ozouville (2010), Characterizing the Galápagos terrestrial climate in the face of global climate change, *Galápagos Research*, *67*, 26-37.

Vailleux, Y., and L. Bourgue (1974), La mise en valeur des eaux souterraines dans l'archipel du Cap Vert [The development of groundwater in the archipelago of Cape Verde], edited, p. 291, BURGEAP, Ministério da Coordenação Interterritorial, Brigada de Águas Subterraneas do Cabo Verde, Paris.

Vaughan, K. L., and P. A. McDaniel (2009), Organic Soils on Basaltic Lava Flows in a Cool, Arid Environment, *Soil Sci. Soc. Am. J.*, *73*(5), 1510-1518.

Violette, S., E. Ledoux, P. Goblet, and J. P. Carbonnel (1997), Hydrologic and thermal modeling of an active volcano: The Piton de la Fournaise, Reunion, *J. Hydrol.*, *191*(1-4), 37-63.

Violette, S., G. De Marsily, J. P. Carbonnel, P. Goblet, E. Ledoux, S. M. Tijani, and G. Vouille (2001), Can rainfall trigger volcanic eruptions? A mechanical stress model of an active volcano: 'Piton de la Fournaise', Reunion Island, *Terra Nova*, *13*(1), 18-24.

Vitousek, P. M. (2004), *Nutrient Cycling and Limitation: Hawai'i as a Model System*, Princeton University Press, Princeton, NJ.

Vitousek, P. M., O. A. Chadwick, P. Matson, S. Allison, L. A. Derry, L. Kettley, A. Luers, E. Mecking, V. Monastra, and S. Porder (2003), Erosion and the rejuvenation of weathering-derived nutrient supply in an old tropical landscape, *Ecosystems*, *6*(762-772).

Webster, J. M., L. M. Wallace, D. A. Clague, and J. C. Braga (2007), Numerical modeling of the growth and drowning of Hawaiian coral reefs during the last two glacial cycles (0--250 kyr), *Geochem. Geophys. Geosyst.*, *8*(3), Q03011, doi:03010.01029/02006GC001415.

Webster, J. M., D. A. Clague, I. D. E. Faichney, P. D. Fullagar, J. R. Hein, J. G. Moore, and C. K. Paull (2010), Early Pleistocene origin of reefs around Lanai, Hawaii, *Earth Planet. Sci. Lett.*, *290*(3-4), 331-339.

Wells, S. G., J. C. Dohrenwend, L. D. McFadden, B. D. Turrin, and K. D. Mahrer (1985), Late Cenozoic landscape evolution on lava flow surfaces of the Cima volcanic field, Mojave Desert, California, *Geol. Soc. Am. Bull.*, *96*(12), 1518-1529.

Wentworth, C. K. (1927), Estimates of marine and fluvial erosion in Hawaii, *J. Geol.*, *35*(2), 117-133.

West, A. J., A. Galy, and M. Bickle (2005), Tectonic and climatic controls on silicate weathering, *Earth Planet. Sci. Lett.*, *235*, 211-228.

Whittaker, R. J., K. A. Triantis, and R. J. Ladle (2008), A general dynamic theory of oceanic island biogeography, *J. Biogeography*, *35*(6), 977-994.

WMO (1998), 1961-1990 Global climate normals (CLINO), Version 1.0, edited, World Meteorological Organization.

Won, J. H., J. W. Kim, G. W. Koh, and J. Y. Lee (2005), Evaluation of hydrogeological characteristics in Jeju Island, Korea, *Geosci. J.*, *9*(1), 33-46.

Wu, S., R. L. Bras, and A. P. Barros (2006), Sensitivity of channel profiles to precipitation properties in mountain ranges, *J. Geophys. Res.*, *111*(F1), F01024.

Yoo, K., and S. M. Mudd (2008), Discrepancy between mineral residence time and soil age: Implications for the interpretation of chemical weathering rates, *Geology*, *36*, 35-38.

Zhong, S., and A. B. Watts (2002), Constraints on the dynamics f mantle plumes from uplift of the Hawaiian Islands, *Earth Planet. Sci. Lett.*, *203*, 105-116.

Table 1. Precipitation seasonality across ocean island regions, as calculated from WMO station climate normals [*WMO*, 1998]. If all months had equal precipitation, each month would represent 8% of the total annual precipitaiton.

Figure 1. Contrasting appearance of weakly and substantially dissected volcanic landscapes, as illustrated by the Hawaiian Islands of Hawai'i and Kaua'i.

Figure 2. Locations of 97 volcanic ocean islands and shield volcanoes with precipitation and age data used to assess the effects of water availability and age on

landscape evolution. The labels indicate regions used as a frequent examples in the text.

Figure 3. Dissection versus representative precipitation rate and age for the 97 volcanoes listed in the Appendix and depicted in Figure 2. Regions used as frequent examples in the text are colored (blue: Hawaii; brown: Oregon Cascades; green: Galápagos; purple: Cape Verde). Representative age is the best estimate for average time since volcanic construction, while representative precipitation rate is the best estimate of spatially-averaged mean annual precipitation. The degree of landscape dissection was visually classified based on digital terrain models and imagery available through Google Maps (http://maps.google.com), with verification, where possible, by maps, photographs, or descriptions in the referenced literature.

Figure 4: Chemical and physical erosion rates on volcanic islands, measured with diverse methods over diverse timescales. Symbol size is scaled by area with erosion rate. Data were collected in the Azores [*Louvat and Allegre*, 1998]; Hawaiian Islands [*Li*, 1988]; Iceland [*Louvat et al.*, 2008]; Reunion [*Louvat and Allegre*, 1997]; and Tahiti [*Hildenbrand et al.*, 2008]. These data show a positive correlation between chemical and total erosion rates, although we note that the chemical erosion rates reported in these studies are derived from fluvial solute fluxes, and therefore do not include subsurface solute fluxes that discharge directly to the ocean.

Figure 5: At left, shaded relief map of the Hawaiian island of Kaua'i, with drainage basins outlined in black. Black circles represent basin-averaged erosion rates since construction of the original volcano topography at ~4 Ma. Color shows modern

mean annual precipitation rates (PRISM Climate Group, 2006, Oregon State University), resampled to 10-meter grid spacing. At right, basin-averaged erosion rates vs. basin-averaged mean annual precipitation rates. Figure modified from Ferrier et al. [2013].

Figure 6. Erosion rates and rock uplift rates on several volcanic islands. Negative uplift rates indicate subsidence. With the exception of Oahu, which is temporarily rising on Hawaii's flexural bulge at about the same rate it is eroding, these islands are far from topographic steady state (1:1 line). Instead, erosion and subsidence work in concert to lower island topography. Uncertainties in erosion rates are ±1 standard error of the mean, and uncertainties in rock uplift rates are reported ranges. Rates in this compilation were inferred by a variety of methods over a variety of timescales, on Hawaii [*Wentworth*, 1927; *Li*, 1988; *Ludwig et al.*, 1991; *Webster et al.*, 2007], Molokai [*Wentworth*, 1927; *Engels et al.*, 2004; *Montaggioni*, 2005; *Webster et al.*, 2010] Oahu [*Wentworth*, 1927; *Doty et al.*, 1981; *Li*, 1988; *Matsuoka et al.*, 1991; *Matsuoka et al.*, 1992; *Grigg and Jones*, 1997; *Hill et al.*, 1997; *Grigg*, 1998], Reunion [*Montaggioni*, 1988; *Louvat and Allegre*, 1997], and Tahiti [*Pirazzoli et al.*, 1985; *Bard et al.*, 1996; *Montaggioni et al.*, 1997; *Hildenbrand et al.*, 2008].

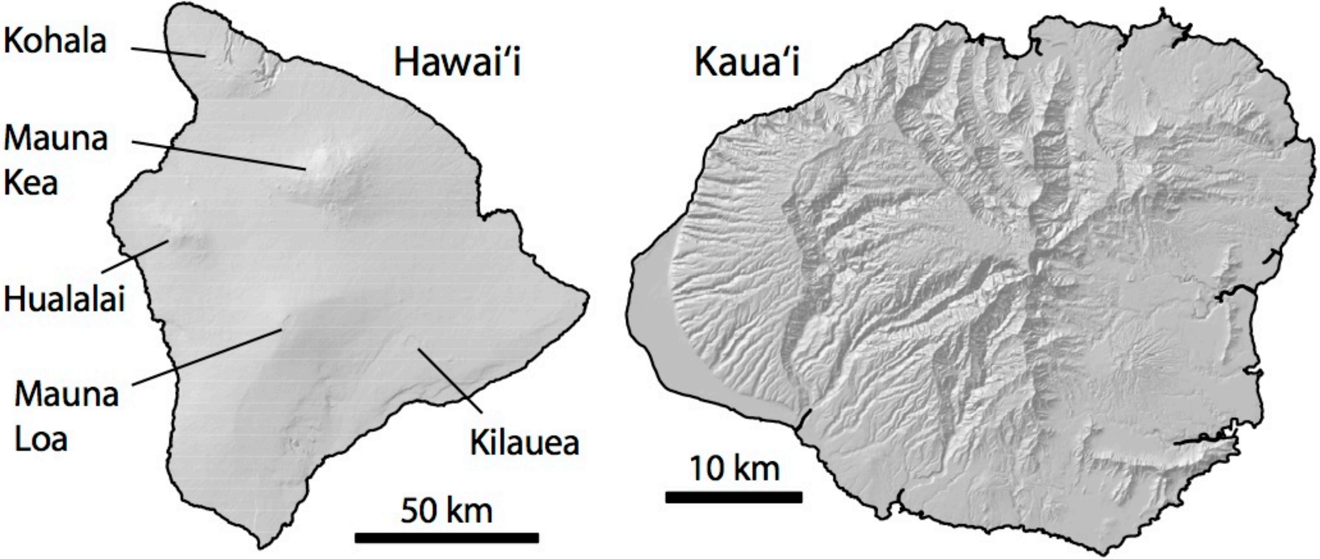
Kohala
Hawai'i
Mauna
Kea
Hualalai
Mauna
Loa
Kilauea
50 km
Kaua'i
10 km

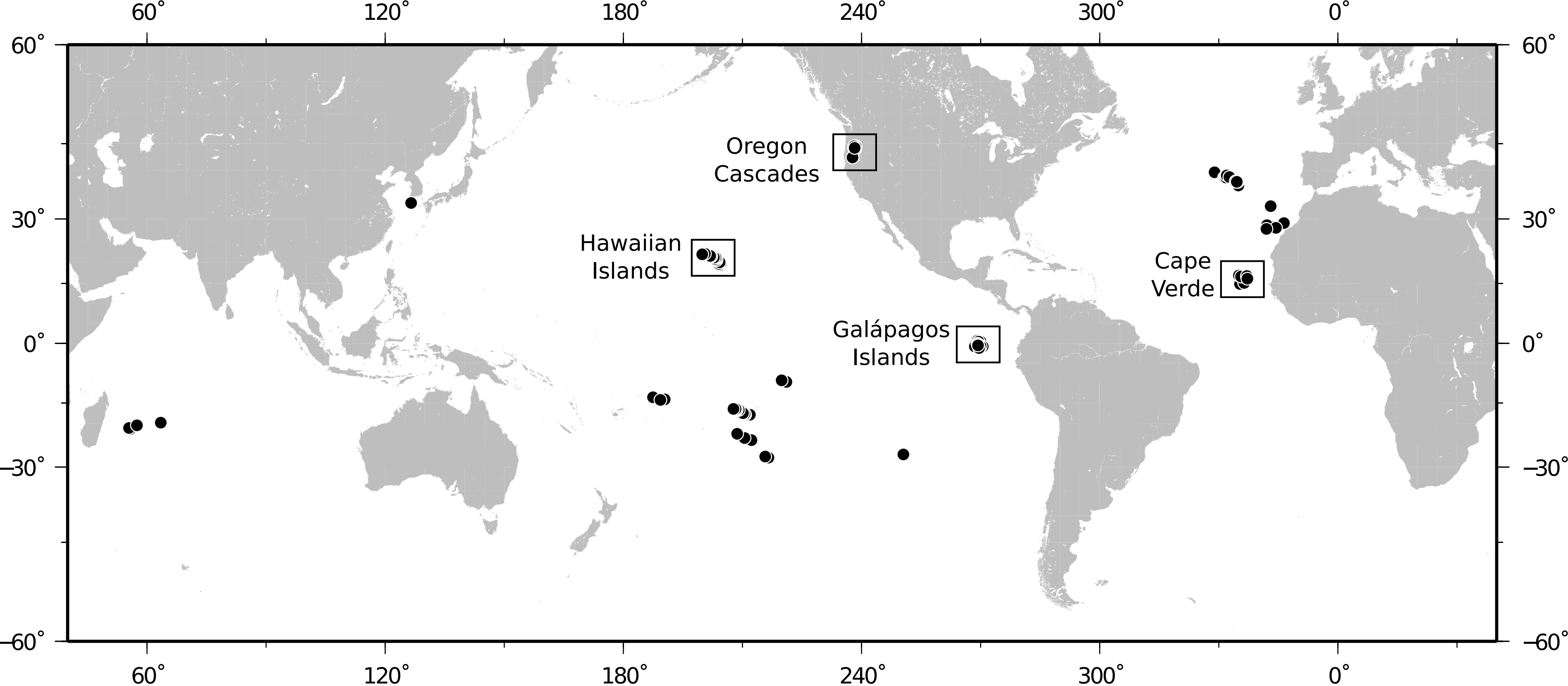

60°
120°
180°
240°
300°
0°
60°
30°
0°
−30°
−60°
Oregon
Cascades
Hawaiian
Islands
Cape
Verde
Galápagos
Islands

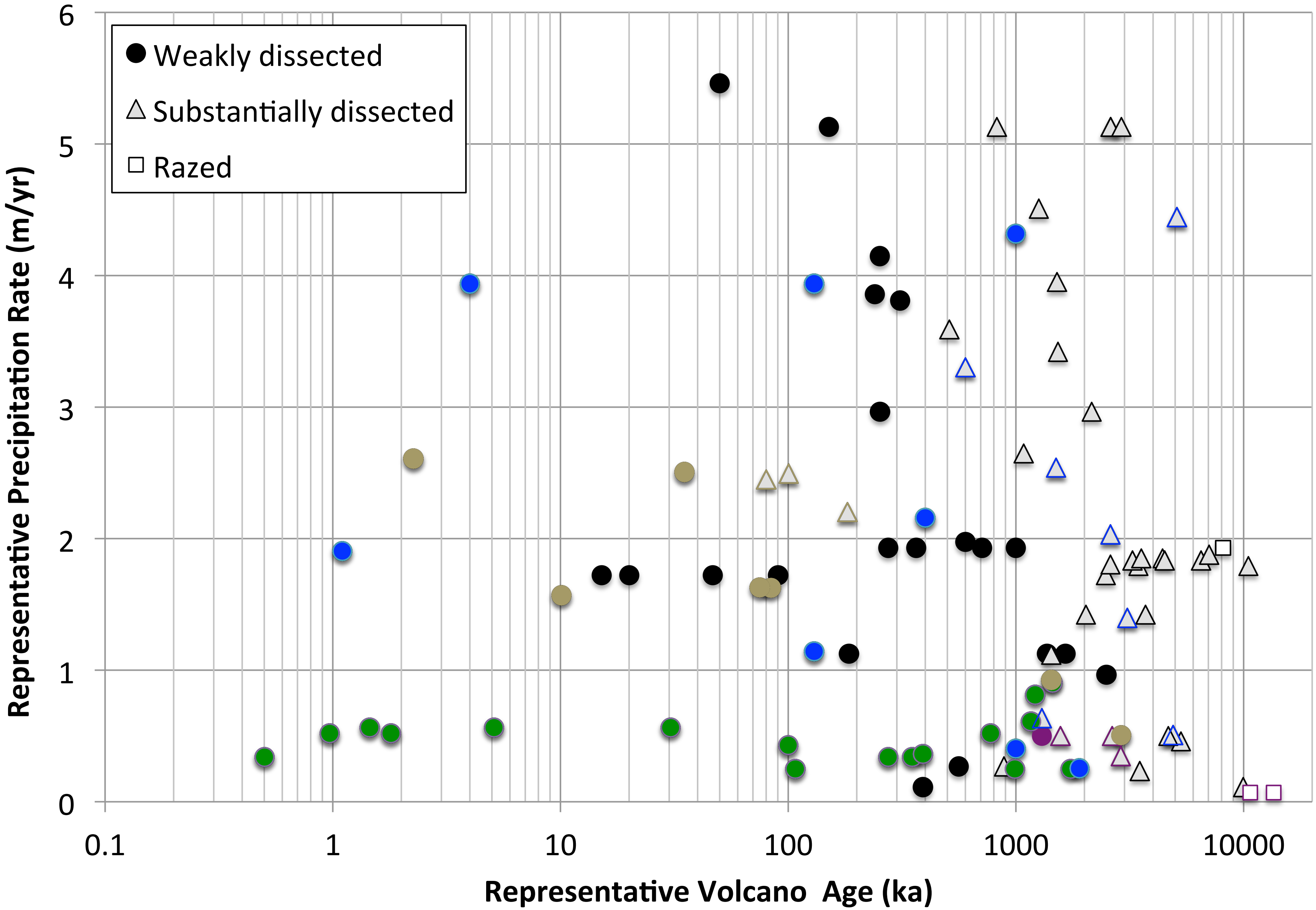
Weakly dissected
Substantially dissected
Razed
Representative Precipitation Rate (m/yr)
0
1
2
3
4
5
6
0.1
1
10
100
1000
10000
Representative Volcano Age (ka)

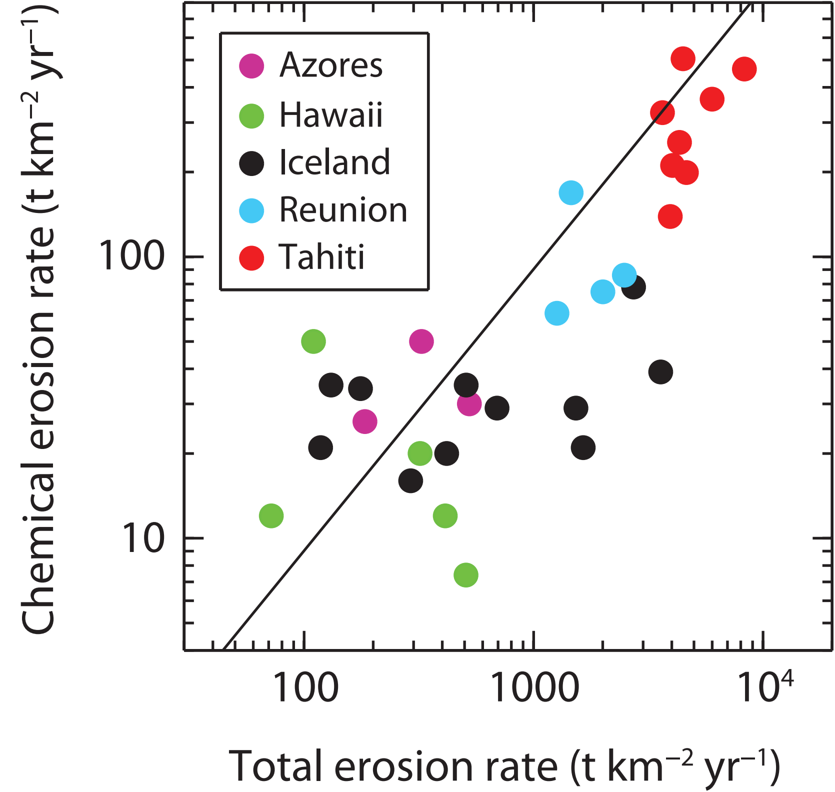

Azores
Hawaii
Iceland
Reunion
Tahiti
100
10
100
1000
10^4
Chemical erosion rate (t km^{-2} yr^{-1})
Total erosion rate (t km^{-2} yr^{-1})

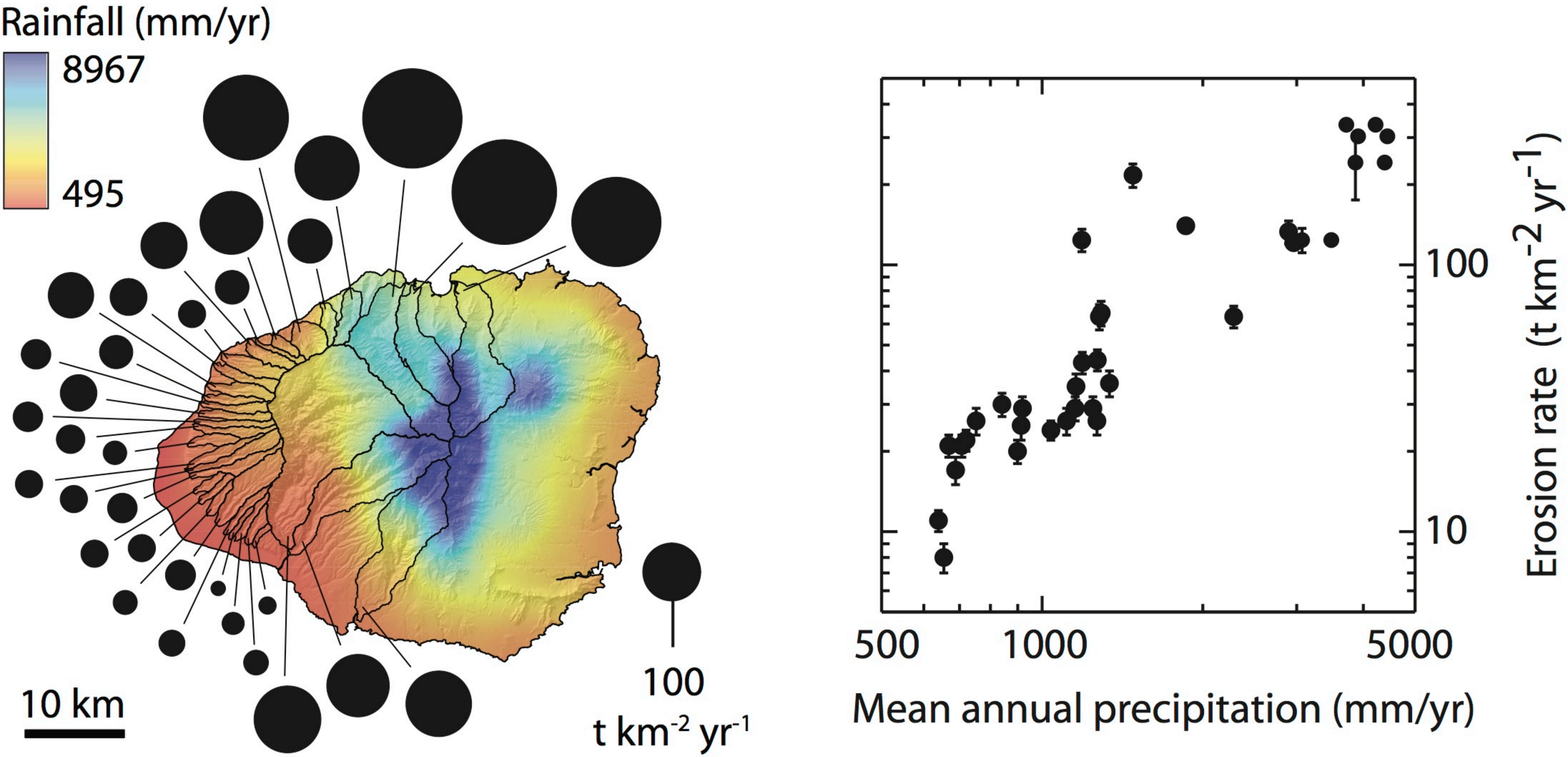

Rainfall (mm/yr)
8967
495
10 km
100
t km^{-2} yr^{-1}
Erosion rate (t km^{-2} yr^{-1})
100
10
500
1000
5000
Mean annual precipitation (mm/yr)

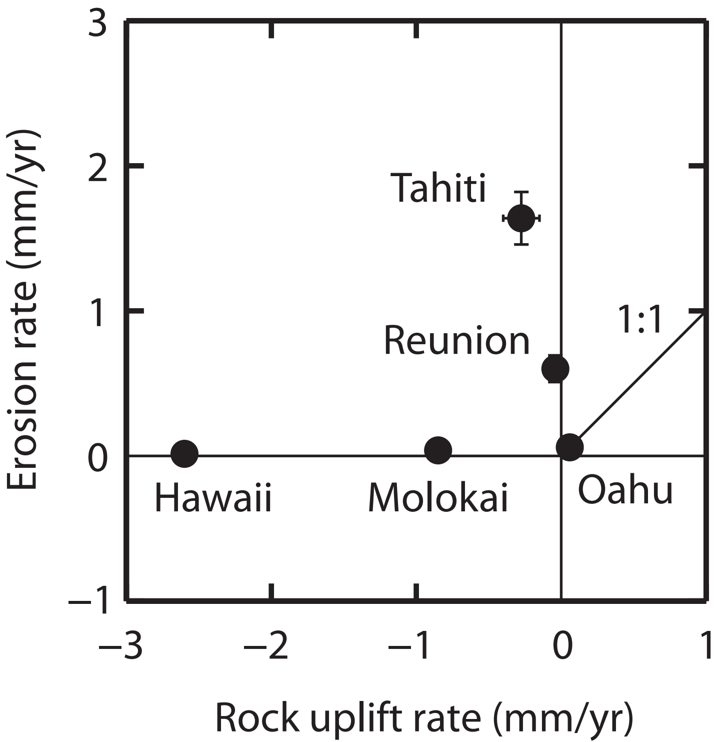

Tahiti
Reunion
1:1
Hawaii
Molokai
Oahu
3
2
1
0
–1
–3
–2
–1
0
1
Erosion rate (mm/yr)
Rock uplift rate (mm/yr)

Table 1. Precipitation seasonality across ocean island regions, as calculated from WMO station climate normals. If all months had equal precipitation, each month would represent 8% of the total annual precipitaiton.

Region	Number of WMO Stations	Average Station Elevation (m)	Max Monthly Precipitation (mm/month)	Max Month Precip / Annual Precip	Min Month Precip / Annual Precip
Austral Is.	2	2	235	0.13	0.05
Azores	3	65	118	0.13	0.03
Canary Is.	3	24	33	0.21	0.00
Cape Verde Is.	1	54	34	0.48	0.00
Easter I.	1	51	153	0.13	0.06
Galápagos Is.	1	6	94	0.21	0.01
Hawaiian Is.	4	19	185	0.16	0.03
Jeju I.	1	22	241	0.17	0.03
Madeira	1	58	103	0.16	0.00
Marquesas	1	51	178	0.13	0.05
Mascarene Is.	2	57	210	0.15	0.03
Society Is.	3	3	370	0.16	0.03

Appendix Table 1. Data sources for calculation of representative age and representative precipitation of 97 shield and ocean island volcanoes. ● indicates weakly dissected; Δ indicates substantially dissected; □ indicates razed morphology.

Volcano Name	Oldest Reported Age (ka)	Youngest Reported Age (ka)	Representative Age (ka)	Maximum Precipitation (m/yr)	Minimum Precipitation (m/yr)	Representative Precipitation (m/yr)	Maximum Elevation (m)
Austral Islands							
Marotiri	**3500**	**3000**	**3250**			**1.83**	**113**
Δ	[*Chauvel et al*., 1997]		Median			Average of Tubuai and Rurutu [*WMO*, 1998]	
Raivavae	**7500**	**5500**	**6500**			**1.83**	**437**
Δ	[*Chauvel et al*., 1997]		Median			Average of Tubuai and Rurutu [*WMO*, 1998]	
Rapa	**5500**	**3500**	**4500**			**1.83**	**650**
Δ	[*Chauvel et al*., 1997]		Median			Average of Tubuai and Rurutu [*WMO*, 1998]	
Rurutu	**13000**	**1100**	**7050**			**1.88**	**385**
Δ	[*Chauvel et al*., 1997]		Median			[*WMO, 1998*] at Rurutu	
Tubuai	**12500**	**8500**	**10500**			**1.79**	**422**
Δ	[*Chauvel et al*., 1997]		Median			[*WMO,* 1998] at Tubuai	
Azores							
Corvo	**1500**	**80**	**710**			**1.93**	**718**
●	[*França et al*., 2006]		[*Cruz et al.*, 2010]			average value for Azores [*Cruz*, 2003]	
Faial	**730**	**0.05**	**365**			**1.93**	**1043**
●	[*Siebert and Simkin*, 2002-]; [*Cruz et al*., 2010]		Median			average value for Azores [*Cruz*, 2003]	
Flores	**2160**	**2.9**	**1081**			**2.65**	**914**
Δ	[*Siebert and Simkin*, 2002-]; [*Cruz et al*., 2010]		Median			[*Cruz*, 2003]	
Fogo	**180**	**0.45**	**90**	**3.00**	**1.00**	**1.72**	**947**
●	[*Moore*, 1990]; [*Siebert and Simkin*, 2002-]		Median	[*Cruz*, 2003]		[*Cruz*, 2003]	
Furnas	**93**	**0.38**	**47**	**2.36**	**1.00**	**1.72**	**805**
●	[*Moore*, 1990]; [*Siebert and Simkin*, 2002-]		Median	[*Cruz et al*., 1999]; [*Cruz*, 2003]		[*Cruz*, 2003]	
Graciosa			**2500**			**0.97**	**402**
●			[*Cruz et al.*, 2010]			[*Cruz*, 2003]	
Nordeste	**4010**	**950**	**2480**	**3.00**	**1.00**	**1.72**	**1103**
Δ	[*Cruz*, 2003]		Median	[*Cruz*, 2003]		[*Cruz*, 2003]	
Pico	**300**	**0.29**	**240**	**7.52**	**1.10**	**3.86**	**2351**
●	[*Cruz and Silva*, 2001]; [*Siebert and Simkin*, 2002-]		[*Cruz and Silva*, 2001]	[*Cruz and Silva*, 2001]		[*Cruz and Silva*, 2001]	

Volcano Name	Oldest Reported Age (ka)	Youngest Reported Age (ka)	Representative Age (ka)	Maximum Precipitation (m/yr)	Minimum Precipitation (m/yr)	Representative Precipitation (m/yr)	Maximum Elevation (m)
Picos	**30**	**0.36**	**15**	**3.00**	**1.00**	**1.72**	**350**
●	[*Moore*, 1990]; [*Siebert and Simkin*, 2002-]		Median	[*Cruz*, 2003]		[*Cruz*, 2003]	
São Jorge	**550**	**0.20**	**275**			**1.93**	**1053**
●	[*Siebert and Simkin*, 2002-]; [*Cruz et al*., 2010]		Median			average value for Azores [*Cruz*, 2003]	
Santa Maria			**8120**			**1.93**	**590**
□			[*Cruz et al.*, 2010]			average value for Azores [*Cruz*, 2003]	
Sete Cidades	**40**	**0.13**	**20**	**3.00**	**1.00**	**1.72**	**856**
●	[*Moore*, 1990]; [*Siebert and Simkin*, 2002-]		Median	[*Cruz*, 2003]		[*Cruz*, 2003]	
Terceira	**2000**	**0.01**	**1000**			**1.93**	**1023**
●	[*Siebert and Simkin*, 2002-]; [*Cruz et al*., 2010]		Median			average value for Azores [*Cruz*, 2003]	
Canary Islands							
El Hierro	**1120**	**2.56**	**561**			**0.27**	**1500**
●	[*Siebert and Simkin*, 2002-]; [*Menendez et al*., 2008]		Median			Average for Canary Islands, based on [*WMO*, 1998] and [*Menendez et al.*, 2008]	
Gran Canaria	**14500**	**1.97**	**5300**	**0.80**	**0.12**	**0.46**	**1950**
Δ	[*Siebert and Simkin*, 2002-]; [*Menendez et al*., 2008]		Onset of rejuvenated volcanism [*Menendez et al.*, 2008]	[*Menendez et al*., 2008]; [*WMO,* 1998] at Las Palmas de Gran Canaria		Median	
La Palma	**1770**	**0.04**	**885**			**0.27**	**2426**
Δ	[*Siebert and Simkin*, 2002-]; [*Menendez et al*., 2008]		Median			Average for Canary Islands, based on [*WMO*, 1998] and [*Menendez et al.*, 2008]	
Lanzarote	**15500**	**0.19**	**7750**			**0.11**	**670**
Δ (●)	[*Siebert and Simkin*, 2002-]; [*Menendez et al*., 2008]		Median			[*WMO,* 1998] at Lanzarote	
Tenerife	**11900**	**0.10**	**3500**			**0.23**	**3715**
Δ	[*Siebert and Simkin*, 2002-]; [*Clarke et al*., 2009]		Onset of renewed volcanism [*Clarke et al.*, 2009]			[*WMO,* 1998] at Santa Cruz de Tenerife	

Volcano Name	Oldest Reported Age (ka)	Youngest Reported Age (ka)	Representative Age (ka)	Maximum Precipitation (m/yr)	Minimum Precipitation (m/yr)	Representative Precipitation (m/yr)	Maximum Elevation (m)
Cape Verde Islands							
Boa Vista	**16630**	**4750**	**10690**			**0.07**	**387**
□	[*Dyhr and Holm*, 2010]		Median			Similar to Sal Island, based on [*WMO*, 1998]	
Brava	**2900**	**240**	**1570**	**1.00**	**0.00**	**0.50**	**900**
Δ	[*Madeira et al.*, 2010]		Median	[*Heilweil et al*., 2009]		Median	
Fogo	**2600**	**0.02**	**1300**	**1.00**	**0.00**	**0.50**	**2829**
●	[*Siebert and Simkin*, 2002-]; [*R. Ramalho*, pers. comm.]		Median	[*Heilweil et al*., 2009]		Median	
Sal Island	**26000**	**1100**	**13550**			**0.07**	**406**
□	[*Torres et al.,* 2002]		Median			[*WMO,* 1998] at Sal Island	
Santiago	**4600**	**700**	**2650**	**1.00**	**0.00**	**0.50**	**1394**
Δ	[*Holm et al*., 2008]		Median	[*Heilweil et al*., 2009]		Median	
São Nicolau	**5710**	**57.8**	**2884**	**0.68**	**0.02**	**0.35**	**1340**
Δ	[*Duprat et al*., 2007]; [*Ramalho et al*., 2010]		Median	[*Heilweil et al*., 2009]		Median	
São Vicente	**9000**	**330**	**4665**	**1.00**	**0.00**	**0.50**	**725**
□	[*Ancochea et al*., 2010]		Median	[*Heilweil et al*., 2009]		Median	
Easter Island							
Poike	**2500**	**800**	**1650**			**1.13**	**370**
●	[*Herrera and Custodio*, 2008]		Median			[*Herrera and Custodio*, 2008]	
Rano Kau	**2560**	**180**	**1370**			**1.13**	**324**
●	[*Herrera and Custodio*, 2008]		Median			[*Herrera and Custodio*, 2008]	
Terevaka	**360**	**10**	**185**			**1.13**	**511**
●	[*Herrera and Custodio*, 2008]		Median			[*Herrera and Custodio*, 2008]	
Galápagos							
Alcedo	**60.8**	**0.03**	**30**	**1.40**	**0.10**	**0.57**	**1130**
●	[*Kurz and Geist*, 1999]; [*Siebert and Simkin*, 2002-]		Median	Based on [*Trueman and d'Ozouville*, 2010]*		Based on [*Trueman and d'Ozouville*, 2010]*	
Cerro Azul	**2.9**	**0.003**	**1**	**1.40**	**0.10**	**0.57**	**1640**
●	[*Kurz and Geist*, 1999]; [*Siebert and Simkin*, 2002-]		Median	Based on [*Trueman and d'Ozouville*, 2010]*		Based on [*Trueman and d'Ozouville*, 2010]*	
Darwin	**1.74**	**0.20**	**1.0**	**1.40**	**0.10**	**0.52**	**1330**
●	[*Kurz and Geist*, 1999]; [*Siebert and Simkin*, 2002-]		Median	Based on [*Trueman and d'Ozouville*, 2010]*		Based on [*Trueman and d'Ozouville*, 2010]*	

Volcano Name	Oldest Reported Age (ka)	Youngest Reported Age (ka)	Representative Age (ka)	Maximum Precipitation (m/yr)	Minimum Precipitation (m/yr)	Representative Precipitation (m/yr)	Maximum Elevation (m)
Ecuador	**127**	**0.86**	**100**	**1.40**	**0.10**	**0.43**	**790**
●	[*Geist et al.*, 2002]; [*Siebert and Simkin*, 2002-]		End of shield-building [*Geist et al.*, 2002]	Based on [*Trueman and d'Ozouville*, 2010]*		Based on [*Trueman and d'Ozouville*, 2010]*	
Fernandina	**1**	**0.002**	**1**	**1.40**	**0.10**	**0.34**	**1496**
●	[*Kurz and Geist*, 1999]; [*Siebert and Simkin*, 2002-]		Median	Based on [*Trueman and d'Ozouville*, 2010]*		Based on [*Trueman and d'Ozouville*, 2010]*	
Floreana	**1520**	**26**	**773**	**1.40**	**0.10**	**0.52**	**640**
●	[*White et al.*, 1993]; [*Kurz and Geist*, 1999]		Median	Based on [*Trueman and d'Ozouville*, 2010]*		Based on [*Trueman and d'Ozouville*, 2010]*	
Genovesa	**350**	**200**	**275**	**0.90**	**0.10**	**0.34**	**64**
●	[*Harpp et al.*, 2002]		Median	Based on [*Trueman and d'Ozouville*, 2010]*		Based on [*Trueman and d'Ozouville*, 2010]*	
Marchena	**560**	**0.01**	**108**	**0.50**	**0.10**	**0.25**	**343**
●	[*White et al.*, 1993]; [*Siebert and Simkin*, 2002-]		Mode of [*White et al.*, 1993]	Based on [*Trueman and d'Ozouville*, 2010]*		Based on [*Trueman and d'Ozouville*, 2010]*	
Pinta	**700**	**0.08**	**350**	**1.40**	**0.10**	**0.34**	**780**
●	[*Cullen and McBirney*, 1987]; [*Siebert and Simkin*, 2002-]		Median	Based on [*Trueman and d'Ozouville*, 2010]*		Based on [*Trueman and d'Ozouville*, 2010]*	
Pinzon	**1400**	**930**	**1165**	**1.40**	**0.10**	**0.61**	**458**
●	[*Swanson et al.*, 1974]; [*White et al.*, 1993]		Median	Based on [*Trueman and d'Ozouville*, 2010]*		Based on [*Trueman and d'Ozouville*, 2010]*	
Rabida	**1060**	**920**	**990**	**0.50**	**0.10**	**0.25**	**367**
●	[*Swanson et al.*, 1974]		Median	Based on [*Trueman and d'Ozouville*, 2010]*		Based on [*Trueman and d'Ozouville*, 2010]*	
San Cristobal	**2300**	**600**	**1450**	**2.00**	**0.50**	**0.91**	**759**
●	[*Geist et al.*, 1986]		Median	[*Adelinet et al.*, 2008]		Based on [*Trueman and d'Ozouville*, 2010]*	
Santa Cruz	**2000**	**585**	**1215**	**1.40**	**0.28**	**0.81**	**864**
●	[*Kurz and Geist*, 1999]; [*Adelinet et al.*, 2008]		Average of [*White et al.*, 1993]	[*Trueman and d'Ozouville*, 2010]		Bellavista station [*Trueman and d'Ozouville*, 2010]	
Santa Fe	**2760**	**720**	**1740**	**0.50**	**0.10**	**0.25**	**260**
●	[*White et al.*, 1993]		Median	Based on [*Trueman and d'Ozouville*, 2010]*		Based on [*Trueman and d'Ozouville*, 2010]*	
Santiago	**780**	**0.11**	**390**	**1.40**	**0.10**	**0.36**	**920**
●	[*Swanson et al.*, 1974]; [*Siebert and Simkin*, 2002-]		Median	Based on [*Trueman and d'Ozouville*, 2010]*		Based on [*Trueman and d'Ozouville*, 2010]*	
Sierra Negra	**10.2**	**0.006**	**5**	**1.40**	**0.10**	**0.57**	**1124**
●	[*Kurz and Geist*, 1999]; [*Siebert and Simkin*, 2002-]		Median	Based on [*Trueman and d'Ozouville*, 2010]*		Based on [*Trueman and d'Ozouville*, 2010]*	
Wolf	**173**	**0.03**	**2**	**1.40**	**0.10**	**0.52**	**1710**
●	[*Siebert and Simkin*, 2002-]; [*Geist et al.*, 2005]		Oldest flank lava [*Geist et al.*, 2005]	Based on [*Trueman and d'Ozouville*, 2010]*		Based on [*Trueman and d'Ozouville*, 2010]*	

Volcano Name	Oldest Reported Age (ka)	Youngest Reported Age (ka)	Representative Age (ka)	Maximum Precipitation (m/yr)	Minimum Precipitation (m/yr)	Representative Precipitation (m/yr)	Maximum Elevation (m)
Hawaiian Islands							
East Molokai	**1530**	**350**	**1500**	**4.06**	**1.02**	**2.54**	**1210**
Δ	[*Clague and Moore*, 2002]		[*Robinson and Eakins*, 2006]	[*Fletcher et al.*, 2002]		Median	
Haleakala		**0.26**	**1000**	**8.38**	**0.25**	**4.32**	**3055**
●	[*Siebert and Simkin*, 2002-]		[*Robinson and Eakins*, 2006]	[*PRISM*, 2012]		Median	
Hualalai	**300**	**0.21**	**130**	**2.03**	**0.25**	**1.14**	**2523**
●	[*JG Moore and Clague*, 1992]; [*Siebert and Simkin*, 2002-]		[*J G Moore and Clague*, 1992]	[*PRISM*, 2012]		Median	
Kahoolawe			**1000**			**0.40**	**1483**
●			[*Robinson and Eakins*, 2006]			1989-2012, station #512558 Kahoolawe 499.6, http://www.wrcc.dri.edu/cgi-bin/cliGCStP.pl?hi2558	
Kilauea	**22.8**	**0**	**1**	**3.05**	**0.76**	**1.91**	**1222**
●	[*Rubin et al.*, 1987]; [*Siebert and Simkin*, 2002-]		[*J G Moore and Clague*, 1992]	[*PRISM*, 2012]		Median	
Kohala	**1159**	**60**	**400**	**4.06**	**0.25**	**2.16**	**1670**
●	[*Lipman and Calvert*, 2011]		[*Robinson and Eakins*, 2006]	[*PRISM*, 2012]		Median	
Koolau		**1830**	**2600**	**3.56**	**0.51**	**2.03**	**945**
Δ	[*Gripp and Gordon*, 2002]		[*Robinson and Eakins*, 2006]	[*PRISM*, 2012]		Median	
Lanai		**1240**	**1300**	**1.02**	**0.25**	**0.64**	**1026**
Δ	[*Gripp and Gordon*, 2002]		[*Robinson and Eakins*, 2006]	[*Fletcher et al.*, 2002]		Median	
Mauna Kea	**240**	**4.47**	**130**	**7.62**	**0.25**	**3.94**	**4205**
●	[*J G Moore and Clague*, 1992]; [*Siebert and Simkin*, 2002-]		[*J G Moore and Clague*, 1992]	[*PRISM*, 2012]		Median	
Mauna Loa	**200**	**0.03**	**4**	**7.62**	**0.25**	**3.94**	**4170**
●	[*J G Moore and Clague*, 1992]; [*Siebert and Simkin*, 2002-]		[*J G Moore and Clague*, 1992]	[*PRISM*, 2012]		Median	
Niihau		**4890**	**4900**	**0.51**	**0.51**	**0.51**	**390**
Δ	[*Gripp and Gordon*, 2002]		[*Robinson and Eakins*, 2006]	[*PRISM*, 2012]		Median	
Olokele (Kaua'i)		**3947**	**5100**	**8.38**	**0.51**	**4.45**	**1593**
Δ	[*Gripp and Gordon*, 2002]		[*Robinson and Eakins*, 2006]	[*PRISM*, 2012]		Median	
Waianae	**3930**	**3080**	**3080**	**2.29**	**0.51**	**1.40**	**1221**
Δ	[*Guillou et al.*, 2000]		[*Guillou et al.*, 2000]	[*PRISM*, 2012]		Median	
West Maui	**1300**	**400**	**600**	**6.35**	**0.25**	**3.30**	**1764**
Δ	[*McDougall*, 1964]; [*Tagami et al.*, 2003]		Onset of rejuvenated volcanism [*Tagami et al.*, 2003]	[*PRISM*, 2012]		Median	

Volcano Name	Oldest Reported Age (ka)	Youngest Reported Age (ka)	Representative Age (ka)	Maximum Precipitation (m/yr)	Minimum Precipitation (m/yr)	Representative Precipitation (m/yr)	Maximum Elevation (m)
West Molokai	**1900**	**1720**	**1900**	**0.51**	**0.00**	**0.25**	**421**
●	[*Clague and Moore*, 2002]		[*Robinson and Eakins*, 2006]	[*Fletcher et al.*, 2002]		Median	
Jeju Island							
Halla	**1200**	**1.0**	**601**	**3.40**	**1.20**	**1.98**	**1950**
●	[*Siebert and Simkin*, 2002-]; [*Won et al.*, 2006]		Median	[*Won et al.*, 2006]		[*Won et al.*, 2006]	
Madeira							
Madeira	**5200**	**6**	**2603**	**2.97**	**0.64**	**1.80**	**1862**
Δ	[*Prada et al.*, 2005]		Median	[*Prada et al.*, 2005]; [*WMO*, 1998] at Funchal		Median	
Marquesas							
Hiva Oa	**2480**	**1580**	**2030**			**1.42**	**1213**
Δ	[*Duncan and McDougall*, 1974]		Median			[*WMO,* 1998] at Atuona, Hiva Oa	
Ua Pou	**5610**	**1800**	**3705**			**1.42**	**1230**
Δ	[*Duncan et al.*, 1986]		Median			[*WMO,* 1998] at Atuona, Hiva Oa	
Mascarene Islands							
Mauritius	**7800**	**170**	**3450**			**1.79**	**828**
Δ	*[McDougall and Chamalaun*, 1969]		Onset of younger volcanic series [*McDougall and Chamalaun*, 1969]			[*WMO*, 1998] at Plaisance	
Piton de la Fournaise	**500**	**5**	**253**	**10.96**	**0.90**	**4.15**	**2632**
●	[*Join et al.*, 2005]		Median	[*Violette et al.*, 1997]		[*Violette et al.*, 1997]	
Piton des Neiges	**3000**	**30**	**1515**	**7.00**	**0.90**	**3.95**	**3069**
Δ	[*Louvat and Allegre*, 1997]		Median	[*Louvat and Allegre*, 1997]; [*Violette et al.*, 1997]		Median	
Rodrigues	**1540**	**1320**	**1430**			**1.12**	**398**
Δ	[*McDougall et al.*, 1965]		Median			[*WMO*, 1998] at Rodrigues	
Oregon Cascades							
Belknap Crater	**3.262**	**1.3**	**2**			**2.61**	**2095**
●	[*Sherrod et al.*, 2004]		Median			[*PRISM*, 2012]**	
Black Butte			**1430**			**0.93**	**1962**
●			[*Sherrod et al.*, 2004]			[*PRISM*, 2012]**	
Little Brother	**153.4**	**47.6**	**101**			**2.50**	**2380**
Δ	[*Schmidt and Grunder*, 2009]		Median			[*PRISM*, 2012]**	
Mt. Bachelor	**12.5**	**7.7**	**10**			**1.57**	**2764**
●	[*Sherrod et al.*, 2004]		Median			[*PRISM*, 2012]**	

Volcano Name	Oldest Reported Age (ka)	Youngest Reported Age (ka)	Representative Age (ka)	Maximum Precipitation (m/yr)	Minimum Precipitation (m/yr)	Representative Precipitation (m/yr)	Maximum Elevation (m)
Mt. McLouglin ●	**125** Based on regional map units [*Sherrod and Smith*, 2000]	**25**	**75** Median			**1.63** [*PRISM*, 2012]**	**2894**
North Sister Δ	**500.8** [*Schmidt and Grunder*, 2009]	**55**	**182** [*Schmidt and Grunder*, 2009]			**2.20** [*PRISM*, 2012]**	**3074**
Scott Mtn. ●			**35** [*Jefferson et al.*, 2010]			**2.51** [*PRISM*, 2012]**	**1859**
Squaw Back Ridge ●			**2900** [*Sherrod et al.*, 2004]			**0.51** [*PRISM*, 2012]**	**1408**
Three Fingered Jack Δ	**140** Based on glacial till stratigraphy [*Sherrod et al.*, 2004]	**20**	**80** Median			**2.45** [*PRISM*, 2012]**	**2391**
Tumalo Mtn. ●	**150** Based on glacial till stratigraphy [*Sherrod et al.*, 2004]	**18**	**84** Median			**1.63** [*PRISM*, 2012]**	**2371**
Samoa							
Ofu & Olosega ●	**560** [*Siebert and Simkin*, 2002-]; [*Koppers et al.*, 2011]	**0.15**	**310** [*McDougall*, 2010]	**4.19** [*PRISM*, 2012]	**3.43**	**3.81** Median	**639**
Savai'i ●	**5290** [*Siebert and Simkin*, 2002-]; [*Koppers et al.*, 2011]	**0.1**	**253** Average of [*McDougall*, 2010]			**2.97** 1971-2000 nationwide normal, http://www.mnre.gov.ws/meteorology/Education/climate.htm	**1858**
Ta'u ●	[*McDougall*, 2010]	**20**	**50** [*McDougall*, 2010]	**7.62** [*PRISM*, 2012]	**3.30**	**5.46** Median	**931**
Tutuila Δ	**1540** [*McDougall*, 1985]	**1010**	**1260** [*McDougall*, 2010]	**6.60** [*PRISM*, 2012]	**2.41**	**4.51** Median	**653**
Upolu Δ	**2780** [*McDougall*, 2010]; [*Koppers et al.*, 2011]	**220**	**2150** [*McDougall*, 2010]			**2.97** 1971-2000 nationwide normal, http://www.mnre.gov.ws/meteorology/Education/climate.htm	**1100**

Volcano Name	Oldest Reported Age (ka)	Youngest Reported Age (ka)	Representative Age (ka)	Maximum Precipitation (m/yr)	Minimum Precipitation (m/yr)	Representative Precipitation (m/yr)	Maximum Elevation (m)
Society Islands							
Bora Bora	**4010**	**3100**	**3555**	**8.50**	**1.91**	**5.20**	**727**
Δ	[*Guillou et al*., 2005]; [*Uto et al*., 2007]		Median	Similar to Tahiti, based on [*Hildenbrand et al*., 2005]; [*WMO,* 1998] at Bora Bora		Median	
Huahine	**3190**	**2020**	**2605**			**5.13**	**669**
Δ	[*Uto et al*., 2007]		Median			Similar to Tahiti, based on [*Hildenbrand et al*., 2005] and [*WMO*, 1998]	
Maupiti	**4610**	**4200**	**4405**			**5.13**	**380**
Δ	[*Guillou et al*., 2005]; [*Uto et al*., 2007]		Median			Similar to Tahiti, based on [*Hildenbrand et al*., 2005] and [*WMO*, 1998]	
Mehetia	**300**	**2**	**151**			**5.13**	**435**
●	[*Siebert and Simkin*, 2002-]; [*Guillou et al*., 2005]		Median			Similar to Tahiti, based on [*Hildenbrand et al*., 2005] and [*WMO*, 1998]	
Moorea	**1700**	**1360**	**1530**			**5.13**	**1207**
Δ	[*Guillou et al*., 2005]		Median			Similar to Tahiti, based on [*Hildenbrand et al*., 2005] and [*WMO*, 1998]	
Raiatea	**2770**	**2440**	**2605**			**5.13**	**1017**
Δ	[*Guillou et al*., 2005]; [*Uto et al*., 2007]		Median			Similar to Tahiti, based on [*Hildenbrand et al*., 2005] and [*WMO*, 1998]	
Tahaa	**3240**	**2570**	**2905**			**5.13**	**590**
Δ	[*Uto et al*., 2007]		Median			Similar to Tahiti, based on [*Hildenbrand et al*., 2005] and [*WMO*, 1998]	
Tahiti	**1400**	**250**	**825**	**8.50**	**1.76**	**5.13**	**2241**
Δ	[*Hildenbrand et al*., 2004]		Median	[*Hildenbrand et al*., 2005]; [*WMO,* 2010] at Faa'a, Tahiti		Median	
Taiarapu (Tahiti-Iti)			**510**			**3.59**	**1306**
Δ			[*Uto et al*., 2007]			[*WMO,* 1998] at Tautiri, Tahiti	

* Estimated based on vegetation zonation and precipitation-vegetation relationships described in [*Trueman and d'Ozouville*, 2010]. Representative precipitation is calculated from the sum of the precipitation in each zone multipled by the fraction of the island covered by that zone.

** [*PRISM,* 2012] for 1971-2000 normal for 800 m cell covering volcano summit

Appendix References Cited

Acosta, J., E. Uchupi, A. Muñoz, P. Herranz, C. Palomo, M. Ballesteros, and ZEE Working Group (2003), Geologic evolution of the Canarian Islands of Lanzarote, Fuerteventura, Gran Canaria and La Gomera and comparison of landslides at these islands with those at Tenerife, La Palma and El Hierro, *Marine Geophysical Researches*, *24*, 1-40.

Adelinet, M., J. Fortin, N. D'Ozouville, and S. Violette (2008), The relationship between hydrodynamic properties and weathering of soils derived from volcanic rocks, Galápagos Islands (Ecuador), *Environ. Geol.*, *56*(1), 45-58.

Ancochea, E., M. J. Huertas, F. Hernan, and J. L. Brandle (2010), Volcanic evolution of Sao Vicente, Cape Verde Islands The Praia Grande landslide, *J. Volcanol. Geotherm. Res.*, *198*(1-2), 143-157.

Chauvel, C., W. McDonough, G. Guille, R. Maury, and R. Duncan (1997), Contrasting old and young volcanism in Rurutu Island, Austral chain, *Chem. Geol.*, *139*, 125-143.

Clague, D. A., and J. G. Moore (2002), The proximal part of the giant submarine Wailau landslide, Molokai, Hawaii, *J. Volcanol. Geotherm. Res.*, *113*(1–2), 259-287.

Clarke, H., V. R. Troll, and J. C. Carracedo (2009), Phreatomagmatic to Strombolian eruptive activity of basaltic cinder cones: Montana Los Erales, Tenerife, Canary Islands, *J. Volcanol. Geotherm. Res.*, *180*(2-4), 225-245.

Cruz, J. V. (2003), Groundwater and volcanoes: examples from the Azores archipelago, *Environ. Geol.*, *44*(3), 343-355.

Cruz, J. V., and M. O. Silva (2001), Hydrogeologic framework of Pico Island, Azores, Portugal, *Hydrogeol. J.*, *9*(2), 177-189.

Cruz, J. V., D. Pacheco, R. Cymbron, and S. Mendes (2010), Monitoring of the groundwater chemical status in the Azores archipelago (Portugal) in the context of the EU water framework directive, *Environ. Earth Sci.*, *61*(1), 173-186.

Cruz, J. V., R. M. Coutinho, M. R. Carvalho, N. Oskarsson, and S. R. Gislason (1999), Chemistry of waters from Furnas volcano, Sao Miguel, Azores: fluxes of volcanic carbon dioxide and leached material, *J. Volcanol. Geotherm. Res.*, *92*(1-2), 151-167.

Cullen, A., and A. R. McBirney (1987), The volcanic geology and petrology of Isla Pinta, Galapagos archipelago, *Geol. Soc. Am. Bull.*, *98*(3), 294-301.

Duncan, R. A., and I. McDougall (1974), Migration of volcanism with time in the Marquesas Islands, French Polynesia, *Earth Planet. Sci. Lett.*, *21*(4), 414-420.

Duncan, R. A., M. T. McCulloch, H. G. Barsczus, and D. R. Nelson (1986), Plume versus lithospheric sources for melts at Ua Pou, Marquesas Islands, *Nature*, *322*(6079), 534-538.

Duprat, H. I., J. Friis, P. M. Holm, T. Grandvuinet, and R. V. Sørensen (2007), The volcanic and geochemical development of São Nicolau, Cape Verde Islands: Constraints from field and 40Ar/39Ar evidence, *J. Volcanol. Geotherm. Res.*, *162*(1-2), 1-19.

Dyhr, C. T., and P. M. Holm (2010), A volcanological and geochemical investigation of Boa Vista, Cape Verde Islands; Ar-40/Ar-39 geochronology and field constraints, *J. Volcanol. Geotherm. Res.*, *189*(1-2), 19-32.

Fletcher, C. H. I., E. E. Grossman, B. M. Richmond, and A. E. Gibbs (2002), Atlas of Natural Hazards in the Hawaiian Coastal Zone *Geol. Invest. Ser. I-2761*, 182 pp, U.S. Geol. Surv., Washington, D.C.

França, Z., M. Lago, J. C. Nunes, C. Galé, V. H. Forjaz, O. Pueyo, and y. E. Arranz (2006), Geochemistry of alkaline basalts of Corvo Island (Azores, Portugal): preliminary data, *Geogaceta*, *40*, 87-90.

Geist, D. J., A. R. McBirney, and R. A. Duncan (1986), Geology and petrogenesis of lavas from San Cristobal Island, Galápagos Archipelago, *Geol. Soc. Am. Bull.*, *97*(5), 555-566.

Geist, D. J., W. M. White, F. Albarede, K. Harpp, R. Reynolds, J. Blichert-Toft, and M. D. Kurz (2002), Volcanic evolution in the Galapagos: The dissected shield of Volcan Ecuador, *Geochem. Geophys. Geosyst.*, *3*(10), 1061.

Geist, D. J., T. R. Naumann, J. J. Standish, M. D. Kurz, K. S. Harpp, W. M. White, and D. J. Fornari (2005), Wolf Volcano, Galápagos Archipelago: Melting and Magmatic Evolution at the Margins of a Mantle Plume, *Journal of Petrology*, *46*(11), 2197-2224.

Gleizal, C. (editor) (1990), *Encyclopédie de la Polynésie,* vol 1, Multipress, Tahiti.

Gripp, A. E., and R. G. Gordon (2002), Young tracks of hotspots and current plate velocities, *Geophys. J. Int.*, *150*(2), 321-361.

Guillou, H., J. Sinton, C. Laj, C. Kissel, and N. Szeremeta (2000), New K–Ar ages of shield lavas from Waianae Volcano, Oahu, Hawaiian Archipelago, *J. Volcanol. Geotherm. Res.*, *96*(3–4), 229-242.

Guillou, H., R. C. Maury, S. Blais, J. Cotten, C. Legendre, G. Guille, and M. Caroff (2005), Age progression along the Society hotspot chain (French Polynesia) based on new unspiked K-Ar ages, *Bull. Soc. Geol. Fr.*, *176*(2), 135-150.

Harpp, K. S., K. R. Wirth, and D. J. Korich (2002), Northern Galapagos Province: Hotspot-induced, near-ridge volcanism at Genovesa Island, *Geology*, *30*(5), 399-402.

Heilweil, V. M., D. K. Solomon, S. B. Gingerich, and I. M. Verstraeten (2009), Oxygen, hydrogen, and helium isotopes for investigating groundwater systems of the Cape Verde Islands, West Africa, *Hydrogeol. J.*, *17*(5), 1157-1174.

Herrera, C., and E. Custodio (2008), Conceptual hydrogeological model of volcanic Easter Island (Chile) after chemical and isotopic surveys, *Hydrogeol. J.*, *16*(7), 1329-1348.

Hildenbrand, A., P. Y. Gillot, and I. Le Roy (2004), Volcano-tectonic and geochemical evolution of an oceanic intra-plate volcano: Tahiti-Nui (French Polynesia), *Earth Planet. Sci. Lett.*, *217*(3-4), 349-365.

Hildenbrand, A., C. Marlin, A. Conroy, P. Y. Gillot, A. Filly, and M. Massault (2005), Isotopic approach of rainfall and groundwater circulation in the volcanic structure of Tahiti-Nui (French Polynesia), *J. Hydrol.*, *302*(1-4), 187-208.

Holm, P. M., T. Grandvuinet, J. Friis, J. R. Wilson, A. K. Barker, and S. Plesner (2008), An Ar-40-Ar-39 study of the Cape Verde hot spot: Temporal evolution in a semistationary plate environment, *J. Geophys. Res.-Solid Earth*, *113*(B8), 22.

Jefferson, A., G. Grant, S. Lewis, and S. Lancaster (2010), Coevolution of hydrology and topography on a basalt landscape in the Oregon Cascade Range, USA., *Earth Surf. Proc. Land.*, *35*(7), 803-816.

Join, J.-L., J.-L. Folio, and B. Robineau (2005), Aquifers and groundwater within active shield volcanoes. Evolution of conceptual models in the Piton de la Fournaise volcano, *J. Volcanol. Geotherm. Res.*, *147*(1-2), 187-201.

Koppers, A. A. P., J. A. Russell, J. Roberts, M. G. Jackson, J. G. Konter, D. J. Wright, H. Staudigel, and S. R. Hart (2011), Age systematics of two young en echelon Samoan volcanic trails, *Geochemistry Geophysics Geosystems*, *12*.

Kurz, M. D., and D. Geist (1999), Dynamics of the Galapagos hotspot from helium isotope geochemistry, *Geochim. Cosmochim. Acta*, *63*(23-24), 4139-4156.

Lipman, P. W., and A. T. Calvert (2011), Early growth of Kohala volcano and formation of long Hawaiian rift zones, *Geology*, *39*(7), 659-662.

Louvat, P., and C. J. Allegre (1997), Present denudation rates on the island of Reunion determined by river geochemistry: Basalt weathering and mass budget between chemical and mechanical erosions, *Geochim. Cosmochim. Acta*, *61*(17), 3645-3669.

Madeira, J., J. Mata, C. Mourao, A. B. da Silveira, S. Martins, R. Ramalho, and D. L. Hoffmann (2010), Volcano-stratigraphic and structural evolution of Brava Island (Cape Verde) based on Ar-40/Ar-39, U-Th and field constraints, *J. Volcanol. Geotherm. Res.*, *196*(3-4), 219-235.

McDougall, I. (1964), Potassium-Argon Ages from Lavas of the Hawaiian Islands, *Geol. Soc. Am. Bull.*, *75*(2), 107-128.

McDougall, I. (1985), Age and evolution of the volcanoes of Tutuila, American Samoa, *Pacific Science*, *39*, 311-320.

McDougall, I. (2010), Age of volcanism and its migration in the Samoa Islands, *Geol. Mag.*, *147*(5), 705-717.

McDougall, I., and F. H. Chamalaun (1969), Isotopic Dating and Geomagnetic Polarity Studies on Volcanic Rocks from Mauritius, Indian Ocean, *Geol. Soc. Am. Bull.*, *80*(8), 1419-1442.

McDougall, I., B. G. J. Upton, and W. J. Wadsworth (1965), A geological reconnaissance of Rodriguez Island, Indian Ocean, *Nature*, *206*(4979), 26-27.

Menendez, I., P. G. Silva, M. Martin-Betancor, F. J. Perez-Torrado, H. Guillou, and S. Scaillet (2008), Fluvial dissection, isostatic uplift, and geomorphological evolution of volcanic islands (Gran Canaria, Canary Islands, Spain), *Geomorphol.*, *102*(1), 189-203.

Moore, J. G., and D. A. Clague (1992), Volcano growth and evolution of the island of Hawaii, *Geol. Soc. Am. Bull.*, *104*(11), 1471-1484.

Moore, R. B. (1990), Volcanic geology and eruption frequency, São Miguel, Azores, *Bull. Volcanol.*, *52*(8), 602-614.

Prada, S. N., M. O. da Silva, and J. Cruz (2005), Groundwater behavior in Madeira, volcanic island (Portugal), *Hydrogeol. J.*, *13*, 800-812.

PRISM (2012), PRISM Climate Group, Oregon State University, in Secondary PRISM Climate Group, Oregon State University, http://prism.oregonstate.edu.

Ramalho, R., G. Helffrich, M. Cosca, D. Vance, D. Hoffmann, and D. N. Schmidt (2010), Vertical movements of ocean island volcanoes: Insights from a stationary plate environment, *Mar. Geol.*, *275*, 84-95.

Robinson, J. E., and B. W. Eakins (2006), Calculated volumes of individual shield volcanoes at the young end of the Hawaiian Ridge, *J. Volcanol. Geotherm. Res.*, *151*(1–3), 309-317.

Rubin, M., L. K. Gargulinski, and J. P. McGeehin (1987), Hawaii radiocarbon dates, in *Volcanism in Hawaii*, edited by R. W. Decker, T. L. Wright and P. H. Stauffer, pp. 213-242, U.S. Geol. Surv. .

Schmidt, M. E., and A. L. Grunder (2009), The evolution of North Sister: A volcano shaped by extension and ice in the central Oregon Cascade Arc, *Geol. Soc. Am. Bull.*, *121*(5-6), 643-662.

Sherrod, D. R., and J. G. Smith (2000), Geologic Map of Upper Eocene to Holocene Volcanic and Related Rocks of the Cascade Range, Oregon, *Geol. Invest. Ser. I-2569*, U.S. Geol. Surv., Washington, D.C.

Sherrod, D. R., E. M. Taylor, M. L. Ferns, W. E. Scott, R. M. Conrey, and G. A. Smith (2004), Geologic Map of the Bend 30- x 60-Minute Quadrangle, Central Oregon, *Geol. Invest. Ser. I-2683*, U.S. Geol. Surv., Washington, D.C.

Siebert, L., and T. Simkin (2002-), Volcanoes of the World: an Illustrated Catalog of Holocene Volcanoes and their Eruptions, Smithsonian Institution, Global Volcanism Program.

Swanson, F. J., H. W. Baitis, J. Lexa, and J. Dymond (1974), Geology of Santiago, Rábida, and Pinzón Islands, Galápagos, *Geol. Soc. Am. Bull.*, *85*(11), 1803-1810.

Tagami, T., Y. Nishimitsu, and D. R. Sherrod (2003), Rejuvenated-stage volcanism after 0.6-m.y. quiescence at West Maui volcano, Hawaii: new evidence from K–Ar ages and chemistry of Lahaina Volcanics, *J. Volcanol. Geotherm. Res.*, *120*(3–4), 207-214.

Torres, P., L. Silva, A. Serralheiro, C. Tassinari, and J. Munhá (2002), Enquadramento geocronológico pelo método K/Ar das principais sequências vulcano-estratigráficas da Ilha do Sal - Cabo Verde, *Garcia de Orta, Serviços Geológicos*, *18*(1-2), 9-13.

Trueman, M., and N. d'Ozouville (2010), Characterizing the Galápagos terrestrial climate in the face of global climate change, *Galápagos Research*, *67*, 26-37.

Uto, K., Y. Yamamoto, M. Sudo, S. Uchiumi, O. Ishizuka, T. Kogiso, and H. Tsunakawa (2007), New K-Ar ages of the Society Islands, French Polynesia, and implications for the Society hotspot feature, *Earth Planets Space*, *59*(7), 879-885.

Violette, S., E. Ledoux, P. Goblet, and J. P. Carbonnel (1997), Hydrologic and thermal modeling of an active volcano: The Piton de la Fournaise, Reunion, *J. Hydrol.*, *191*(1-4), 37-63.

White, W. M., A. R. McBirney, and R. A. Duncan (1993), Petrology and Geochemistry of the Gal·pagos Islands: Portrait of a Pathological Mantle Plume, *J. Geophys. Res.*, *98*(B11), 19533-19563.

WMO (1998), 1961-1990 Global climate normals (CLINO), Version 1.0, World Meteorological Organization.

Won, J.-H., J.-Y. Lee, J.-W. Kim, and G.-W. Koh (2006), Groundwater occurrence on Jeju Island, Korea, *Hydrogeol. J.*, *14*(4), 532-547.